Accepted Manuscript

2-Aryl-5-amino-1,2,3-triazoles: New effective blue-emitting fluorophores

Kseniya D. Gavlik, Ekaterina S. Sukhorukova, Yuri M. Shafran, Pavel A. Slepukhin, Enrico Benassi, Nataliya P. Belskaya

Please cite this article as: Gavlik KD, Sukhorukova ES, Shafran YM, Slepukhin PA, Benassi E, Belskaya NP, 2-Aryl-5-amino-1,2,3-triazoles: New effective blue-emitting fluorophores, *Dyes and Pigments* (2016), doi: 10.1016/j.dyepig.2016.08.015.

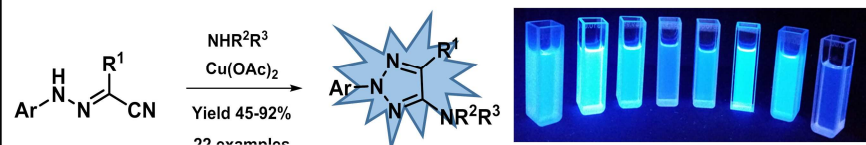# 2-Aryl-5-amino-1,2,3-triazoles: New Effective Blue-Emitting Ffluorophores

Leave this area blank for abstract info.

Kseniya D. Gavlik, Ekaterina S. Sukhorukova, Yuri M. Shafran, Pavel A. Slepukhin, Enrico Benassi, Nataliya P. Belskaya

Ural Federal University, 19 Mira Str., Yekaterinburg 620002, Russia
I. Ya. Postovsky Institute of Organic Synthesis, 20 S. Kovalevskaya Str., Yekaterinburg 620219, Russia
Scuola Normale Superiore, Piazza dei Cavalieri 7, 56126 Pisa, Italy

Highlights

- One-pot synthesis of a series of new 2-aryl-5-amino-1,2,3-triazole derivatives;

- Experimental and computational approaches to optical properties correlate well;

- High photoluminescence quantum yield (99.6%) was achieved;

- Fluorescent properties can be tuned varying the substituents in 1,2,3-triazoles.

2-Aryl-5-amino-1,2,3-triazoles: New Effective Blue-Emitting Fluorophores

Kseniya D. Gavlik [a], Ekaterina S. Sukhorukova [a], Yuri M. Shafran [a], Pavel A. Slepukhin [a,b], Enrico Benassi [c, *], Nataliya P. Belskaya [a, *]

[a]Ural Federal University, 19 Mira Str., Yekaterinburg 620002, Russia
[b]I. Ya. Postovsky Institute of Organic Synthesis, S. Kovalevskaya 20, Yekaterinburg 620219, Russia
[c]Scuola Normale Superiore, Piazza dei Cavalieri 7, 56126 Pisa, Italy

ABSTRACT

The synthesis of a new series of 2-aryl-5-amino-1,2,3-triazole derivatives is reported. The photochemical properties of these new fluorophores were studied both experimentally and using theoretical models. The compounds were found to be fluorescent, with Stokes shifts ranging from 40 nm (2494 см$^{-1}$) to 140 nm (9461 cm^{-1}) and quantum yield values between 0.004 and 0.996. The fluorescence of the 1,2,3-triazoles was highly structure dependent and could be tuned by variation of the substituents at the C-4 and C-5 atoms of triazole ring and by the electronic and spatial effect of substituents within the aromatic cycle. Photophysical studies showed moderate changes in the fluorescence quantum yields depending on the solvent polarity. The UV-Vis spectra calculations employing the time-dependent density functional theory (TD-DFT) are in good agreement with the experimental data. The favourable photophysical properties of the studied compounds and their facile and high-yielding synthesis make them excellent candidates for commercial application as fluorescent tags.

Keywords:

2-Aryl-5-amino-1,2,3-triazole

Fluorescence

Stokes shift

Quantum yield

Solvatochromism

1. Introduction

The design of new fluorescence molecular systems should incorporate synthetic simplicity, structural variability and excellent photophysical properties. Widespread availability, synthetic flexibility and the capacity to easily adjust the conjugation system or molecular electronic structure could facilitate the rapid expansion and straightforward tuning of these fluorophores to promote unique optical and physical properties and develop them for practical applications [1,2]. 1,2,3-triazoles are attractive small molecular weight fluorophores because their heterocyclic core is a popular building-block in medicine, biochemistry and materials chemistry applications [3-7]. Notably, 1,2,3-triazoles have been disclosed as suitable linkers or spacers in biological systems because they are stable to metabolic degradation and are capable of hydrogen bonding or covalent attachment to biomolecule targets [8]. It has been established that the 1,2,3-triazole ring not only functions as a linker between two or more molecular fragments, but it also contributes to the overall physical and chemical properties of the entire molecule.

It is well known that 1-aryl-1,2,3-triazoles are easily accessible via copper(I)-catalyzed cycloaddition between acetylene and azide (CuAAC) [9]. However, the synthesis of isomeric 2-aryl-1,2,3-triazoles is not as simple and often requires laborious synthetic method development or separation from the 1-aryl-1,2,3-triazole isomers [10]. While both N(1)-aryl-1,2,3-triazoles and N(2)-aryl-1,2,3-triazoles absorb under excitation at 330 nm, only the N(2)-analogues exhibit strong fluorescence emission in the UV/blue range with high efficiency in various solvents [11-18]. Although many fluorophores have been developed in recent years, effective UV/blue light-emitting small molecules are rare due to the relatively large energy gap between the interacting orbitals. Meanwhile, the thriving research areas of OLED display and Forster resonance energy transfer studies have increased the demand for effective UV/blue light-emitting molecules [16].

Previously, we reported a one-pot synthesis of 2-aryl-1,2,3-triazoles **1** by a sequence of nucleophilic additions of amines to easily available arylhydrazones bearing nitrile functionality, followed by oxidative cyclization of the formed arylhydrazonoacetamidines [19]. The wide availability

3

of starting compounds, safe synthetic procedures, large yield and simple purification give this method distinct advantages over other systems [19,20]. Additionally, the method is very versatile, as various functional groups (e.g., cyano, benzoyl, alkoxycarbonyl and primary, secondary or tertiary amino) and substituents can be introduced in the triazole and aromatic rings, in contrast to other reported procedures [10].

Herein, we report the design and synthesis of new 2-aryl-5-amino-1,2,3-triazoles and the study of their photophysical properties by experimental and theoretical methods. The study also revealed the structural factors and solvent effects that contribute to the observed fluorescent properties.

2. Experimental

2.1. General information and materials

All reactants were obtained from Acros Organics and used without further purification. ^{1}H NMR and ^{13}C NMR spectra were recorded with a Bruker Avance II (Karlsruhe, Germany) (400 MHz for ^{1}H, 100 MHz for ^{13}C) spectrometer. Chemical shifts are reported in parts per million (ppm) relative to TMS in ^{1}H NMR and to the residual solvent signals in ^{13}C NMR spectra. Coupling constants (J) values are given in Hertz (Hz). Signal splitting patterns are described as a singlet (s), doublet (d), triplet (t), quartet (q), sextet (sext), quintet (quin), multiplet (m), broad (br), doublet of doublets (dd), doublet of triplets (dt) or AA'XX' - spin system of *para*-substituted benzene with two different substituents. The ^{13}C NMR signal patterns for several compounds were analyzed by APT (attached proton test) and are described as follows: + for secondary or quaternary carbon atom (positive signal), - for primary or tertiary carbon atom (negative signal). Mass spectra were recorded with a Shimadzu GCMS-QP 2010 "Ultra" (Kyoto, Japan) mass spectrometer using the electron impact (EI) ionization technique (40-200 °C, 70 eV). The abbreviation [M]$^+$ refers to the molecular ion. The Fourier-transform infrared (FTIR) spectra were obtained using a Bruker Alpha (NPVO, ZnSe) spectrometer (Ettlingen, Germany). Elemental analyses were carried out using a CHNS/O analyzer Perkin-Elmer 2400 Series II instrument

4

(Shelton, CT USA). Melting points were determined on a Stuart SMP3 apparatus (Staffordshire, ST15 OSA, UK). The reactions were monitored by analytical thin-layer chromatography (TLC) on aluminium-backed silica-gel plates (Sorbfil UV–254). Visualization of components was accomplished by short wavelength UV-light (254 nm). Solvents were dried and distilled according to the common procedures. All solvents were of spectroscopic grade.

The title products were purified by column chromatography on silica gel (0.035–0.070, 60 Å) and recrystallized from ethanol.

2.2. Synthesis

2-Aryl-1,2,3-triazoles **4** were prepared by the one-port procedure reported in previous article [19].

General procedure for the synthesis of triazoles 4a-v. A solution of arylhydrazonoyl cyanide **1a-o** (1.0 mmol) and amine **2a-i** (1.5 mmol) in MeCN (10 mL) was heated under reflux for 10 min. Then $Cu(AcO)_2 \cdot H_2O$ (100 mg, 0.5 mmol) was added and the reaction mixture was refluxed for 2-17 h at open air atmosphere, until TLC indicated total consumption of starting hydrazone. The solution was cooled to room temperature and poured into a mixture of water and crushed ice. The resulting precipitate was filtered off and crystallized from ethanol.

*2.2.1. 2-(3,4-Dimethoxyphenyl)-5-(pyrrolidin-1-yl)-2H-1,2,3-triazole-4-carbonitrile (**4a**).* Colorless powder, yield: 260 mg (87%), mp 157-158 °C. FTIR ν_{max} (cm^{-1}) 2984, 2960, 2910, 2840 (CH), 2220 (CN). ^{1}H NMR (CDCl$_3$, 400 MHz): δ 1.93-2.15 (m, 4H, CH$_2$), 3.51-3.70 (m, 4H, CH$_2$), 3.94 (s, 3H, CH$_3$O), 3.98 (s, 3H, CH$_3$O), 6.91 and 7.54 (AA'XX', *J* = 8.4 Hz, 4H, CH$_{Ar}$). ^{13}C NMR (CDCl$_3$, 100 MHz): δ 25.5 (2CH$_2$), 48.5 (2CH$_2$), 56.2 (2CH$_3$O), 96.1, 102.8, 105.5, 111.0, 111.1, 114.2 (CN), 133.0, 149.0, 149.4, 156.1. Found: C, 60.4; H, 5.6; N 23.5%; C$_{15}$H$_{17}$N$_5$O$_2$ requires C, 60.2; H 5.7; N 23.4%. MS-EI m/z: 299 [M]$^+$.

*2.2.2. 2-(4-Methoxyphenyl)-5-(pyrrolidin-1-yl)-2H-1,2,3-triazole-4-carbonitrile (**4b**).* Colorless powder, yield: 247 mg (92%), mp 126-127 °C. FTIR, ν_{max}, cm^{-1}: 2980, 2940, 2883, 2840 (C-H), 2221 (CN). ^{1}H NMR (DMSO-d$_6$, 400 MHz): δ 1.94-1.99 (m, 4H, CH$_2$), 3.47-3.52 (m, 4H, CH$_2$), 3.81 (s, 3H,

5

OCH$_3$), 7.11 and 7.85 (AA'XX', J = 9.3 Hz, 4H, CH$_{Ar}$). ^{13}C NMR APT (DMSO-d$_6$, 100 MHz): δ 25.5 (+) (2CH$_2$), 48.7 (+) (2CH$_2$), 56.0 (-) (CH$_3$O), 105.3 (+), 114.4 (+) (CN), 115.2 (-) (2CH$_{Ar}$), 120.1 (-) (2CH$_{Ar}$), 132.5 (+), 158.2 (+), 159.7 (+). Found: C, 62.2; H, 5.5; N 26.2%; C$_{14}$H$_{15}$N$_5$O requires C, 62.4; H 5.6; N 26.0%. MS-EI m/z: 269 [M]$^+$.

*2.2.3. 2-Phenyl-5-(pyrrolidin-1-yl)-2H-1,2,3-triazole-4-carbonitrile (**4c**).* Colorless powder, yield: 191 mg (80%), mp 102-103 °C. FTIR, v$_{max}$, cm^{-1}: 2980, 2940, 2875 (C-H), 2230 (CN). ^{1}H NMR (DMSO-d$_6$, 400 MHz): δ 1.83-2.02 (m, 4H, CH$_2$), 3.37-3.53 (m, 4H, CH$_2$), 7.44 (t, J = 7.8 Hz, 1H, CH$_{Ar}$), 7.55 (t, J = 7.8 Hz, 2H, CH$_{Ar}$), 7.90 (d, J = 7.8 Hz, 2H, CH$_{Ar}$). ^{13}C NMR APT (DMSO-d$_6$, 100 MHz): δ 25.4 (+) (2CH$_2$), 48.6 (+) (2CH$_2$), 106.1 (+), 114.2 (+) (CN), 118.8 (-) (2CH$_{Ar}$), 128.8 (-) (CH$_{Ar}$), 130.1 (-) (2CH$_{Ar}$), 138.7 (+), 156.0 (+). Found: C, 65.1; H, 5.6; N 29.4%; C$_{13}$H$_{13}$N$_5$ requires C, 65.3; H 5.5; N 29.3%. MS-EI m/z: 239 [M]$^+$.

*2.2.4. 2-(4-Fluorophenyl)-5-(pyrrolidin-1-yl)-2H-1,2,3-triazole-4-carbonitrile (**4d**).* Colorless powder, yield: 216 mg (84%), mp 90-91 °C. FTIR, v$_{max}$, cm^{-1}: 2984, 2967, 2871, 2840 (C-H), 2220 (CN). ^{1}H NMR (CDCl$_3$, 400 MHz): δ 1.95-2.15 (m, 4H, CH$_2$), 3.61 (t, J = 6.6 Hz, 4H, CH$_2$), 7.16 (t, J = 8.6 Hz, 2H, CH$_{Ar}$), 7.98 (dd, J = 4.7, 8.6 Hz, 2H, CH$_{Ar}$). ^{13}C NMR (CDCl$_3$, 100 MHz): δ 25.5 (2CH$_2$), 48.7 (2CH$_2$), 106.3, 113.9 (CN), 116.1 (d, ^2J = 23.1 Hz, 2CH$_{Ar}$), 120.5 (d, ^3J = 8.5 Hz, 2CH$_{Ar}$), 135.4 (d, ^4J = 2.9 Hz, C$_{Ar}$), 156.1, 162.0 (d, ^1J = 246.7 Hz, C$_{Ar}$). Found: C, 60.6; H, 4.7; N 27.3%; C$_{13}$H$_{12}$FN$_5$ requires C, 60.7; H 4.7; N 27.2%. MS-EI m/z: 257 [M]$^+$.

*2.2.5. 2-(4-Chlorophenyl)-5-(pyrrolidin-1-yl)-2H-1,2,3-triazole-4-carbonitrile (**4e**).* Colorless powder, yield: 229 mg (84%), mp 81-82 °C. FTIR, v$_{max}$, cm^{-1}: 2992, 2964, 2870 (C-H), 2221 (CN). ^{1}H NMR (CDCl$_3$, 400 MHz): δ 2.06 (4H, t, J = 6.6 Hz, CH$_2$), 3.61 (4H, t, J = 6.6 Hz, CH$_2$), 7.44 and 7.94 (4H, AA′XX′, J = 8.8 Hz, CH$_{Ar}$). ^{13}C NMR APT (CDCl$_3$, 100 MHz): δ 25.5 (+) (2CH$_2$), 48.5 (+) (2CH$_2$), 106.6 (+), 113.8 (+) (CN), 119.9 (-) (2CH$_{Ar}$), 129.4 (-) (2CH$_{Ar}$), 133.6 (+), 137.6 (+), 156.0 (+). Found: C, 56.8; H, 4.6; N 25.5%; C$_{13}$H$_{12}$ClN$_5$ requires C, 57.0; H 4.4; N 25.6%. MS-EI m/z: 273 [M]$^+$.

*2.2.6.   2-(3,5-Difluorophenyl)-5-(pyrrolidin-1-yl)-2H-1,2,3-triazole-4-carbonitrile   (**4f**).* Colorless powder, yield: 248 mg (90%), mp 124-125 °C. FTIR, ν_{max}, cm^{-1}: 2984, 2980, 2876, 2840 (C-H), 2221 (CN). ^{1}H NMR (DMSO-d$_6$, 400 MHz): δ 1.88-2.06 (m, 4H, CH$_2$), 3.37-3.56 (m, 4H, CH$_2$), 7.34 (t, J = 9.2 Hz, 1H, CH$_{Ar}$), 7.50 (d, J = 6.8 Hz, 2H, CH$_{Ar}$). ^{13}C NMR APT (DMSO-d$_6$, 100 MHz): δ 25.4 (+) (2CH$_2$), 48.6 (+) (2CH$_2$), 102.6 (-) (d, ^2J = 30.1 Hz, 2CH$_{Ar}$), 104.0 (-) (t, ^2J = 25.8 Hz, CH$_{Ar}$), 107.8 (+), 113.5 (+) (CN), 140.4 (+) (t, ^3J = 13.1 Hz, C$_{Ar}$), 156.0 (+), 163.2 (+) (dd, ^1J = 231.4, ^3J = 14.5 Hz, 2C$_{Ar}$). Found: C, 57.0; H, 4.2; N 25.2%; C$_{13}$H$_{11}$F$_2$N$_5$ requires C, 56.7; H 4.0; N 25.4%. MS-EI m/z: 275 [M]$^+$.

*2.2.7.   5-(Pyrrolidin-1-yl)-2-(3-(trifluoromethyl)phenyl)-2H-1,2,3-triazole-4-carbonitrile   (**4g**).* Colorless powder, yield: 240 mg (78%), mp 115-116 °C. FTIR, ν_{max}, cm^{-1}: 2980, 2964, 2888, 2870 (C-H), 2228 (CN). ^{1}H NMR (DMSO-d$_6$, 400 MHz): δ 1.86-2.15 (m, 4H, CH$_2$), 3.40-3.74 (m, 4H, CH$_2$), 7.69-7.95 (m, 2H, CH$_{Ar}$), 8.00-8.14 (m, 1H, CH$_{Ar}$), 8.14-8.37 (m, 1H, CH$_{Ar}$). ^{13}C NMR (DMSO-d$_6$, 100 MHz): δ 24.8 (+) (2CH$_2$), 48.0 (+) (2CH$_2$), 106.7 (+), 113.1 (+), 114.5 (-) (q, ^3J = 4.1 Hz, CH$_{Ar}$), 122.0 (-) (CH$_{Ar}$), 124.5 (-) (q, ^3J = 3.6 Hz, CH$_{Ar}$), 130.3 (+) (q, ^2J = 32.3 Hz), 131.1 (-) (CH$_{Ar}$), 138.4 (+), 155.5 (+). Found: C, 54.9; H, 3.8; N 22.9%; C$_{14}$H$_{12}$F$_3$N$_5$ requires C, 54.7; H 3.9; N 22.8%. MS-EI m/z: 307 [M]$^+$.

*2.2.8. 2-(4-Cyanophenyl)-5-(pyrrolidin-1-yl)-2H-1,2,3-triazole-4-carbonitrile (**4h**).* Colorless powder, yield: 193 mg (73%), mp 167-168 °C. FTIR, ν_{max}, cm^{-1}: 2980, 2956, 2934, 2864 (C-H), 2226 (CN). ^{1}H NMR (CDCl$_3$, 400 MHz): δ 2.00-2.15 (m, 4H, CH$_2$), 3.56-3.71 (m, 4H, CH$_2$), 7.77 and 811 (AA′XX′, J = 7.1 Hz, 4H, CH$_{Ar}$). ^{13}C NMR (CDCl$_3$, 100 MHz): δ 25.5 (2CH$_2$), 48.5 (2CH$_2$), 108.4, 111.2, 113.3 (CN), 118.1, 119.0 (2CH$_{Ar}$), 133.5 (2CH$_{Ar}$), 141.5, 155.9. Found: C, 63.8; H, 4.7; N 31.6%; C$_{14}$H$_{12}$N$_6$ requires C, 63.6; H 4.6; N 31.8%. MS-EI m/z: 264 [M]$^+$.

*2.2.9.   2-(2-Methoxyphenyl)-5-(pyrrolidin-1-yl)-2H-1,2,3-triazole-4-carbonitrile   (**4i**).* Colorless powder, yield: 210 mg (78%), mp 107-108 °C. FTIR, ν_{max}, cm^{-1}: 2970, 2860, 2855 (C-H), 2224 (CN). ^{1}H NMR (CDCl$_3$, 400 MHz): δ 1.97-2.08 (m, 4H, CH$_2$), 3.61 (dd, J = 7.8, 5.5 Hz, 4H, CH$_2$), 3.89 (s,

3H, OCH$_3$), 7.03-7.12 (m, 2H, CH$_{Ar}$), 7.40-7.47 (m, 1H, CH$_{Ar}$), 7.51 (dd, J = 7.8, 1.6 Hz, 1H, CH$_{Ar}$).

^{13}C NMR (CDCl$_3$, 100 MHz): δ 25.5 (2CH$_2$), 48.5 (2CH$_2$), 56.3 (CH$_3$O), 106.3, 112.9, 114.1, 120.7, 126.9, 129.2, 130.9, 153.6, 155.9. Found: C, 62.2; H, 5.7; N 26.1%; C$_{14}$H$_{15}$N$_5$O requires C, 62.4; H 5.6; N 26.0%. MS-EI m/z: 269 [M]$^+$.

2.2.10. 2-(2-Chlorophenyl)-5-(pyrrolidin-1-yl)-2H-1,2,3-triazole-4-carbonitrile (4j). Colorless powder, yield: 210 mg (77%), mp 78-79 °C. FTIR, ν$_{max}$, cm^{-1}: 2982, 2946, 2880, 2840 (C-H), 2220 (CN). ^{1}H NMR (CDCl$_3$, 400 MHz): δ 1.97-2.16 (m, 4H, CH$_2$), 3.62 (t, J = 6.7 Hz, 4H, CH$_2$), 7.38-7.49 (m, 2H, CH$_{Ar}$), 7.51-7.67 (m, 2H, CH$_{Ar}$). ^{13}C NMR (CDCl$_3$, 100 MHz): δ 25.5 (2CH$_2$), 48.5 (2CH$_2$), 107.0, 113.7, 127.4 (CH$_{Ar}$), 127.5 (CH$_{Ar}$), 129.3, 130.5 (CH$_{Ar}$), 131.2 (CH$_{Ar}$), 137.4, 155.9. Found: C, 57.2; H, 4.5; N 25.8%; C$_{13}$H$_{12}$ClN$_5$ requires C, 57.0; H 4.4; N 25.6%. MS-EI m/z: 273 [M]$^+$.

2.2.11. 2-(2,6-Dichlorophenyl)-5-(pyrrolidin-1-yl)-2H-1,2,3-triazole-4-carbonitrile (4k). Colorless powder, yield: 240 mg (78%), mp 103-104 °C. FTIR, ν$_{max}$, cm^{-1}: 2982, 2960, 2890 (C-H), 2221 (CN). ^{1}H NMR (CDCl$_3$, 400 MHz) δ 1.99-2.16 (m, 4H, CH$_2$), 3.62 (t, J = 6.7 Hz, 4H, CH$_2$), 7.40-7.54 (m, 4H, CH$_{Ar}$). ^{13}C NMR (CDCl$_3$, 100 MHz): δ 25.5 (2CH$_2$), 48.5 (2CH$_2$), 106.3, 112.9, 114.1, 120.7, 126.9, 129.2, 130.9, 153.6, 155.9. Found: C, 50.4; H, 3.8; N 22.9%; C$_{13}$H$_{11}$Cl$_2$N$_5$ requires C, 50.7; H 3.6; N 22.7%. MS-EI m/z: 307 [M]$^+$.

2.2.12. 5-(Pyrrolidin-1-yl)-2-(2-(trifluoromethyl)phenyl)-2H-1,2,3-triazole-4-carbonitrile (4l). Colorless powder, yield: 246 mg (80%), mp 93-94 °C. FTIR, ν$_{max}$, cm^{-1}: 2980, 2946, 2882, 2840 (C-H), 2222 (CN). ^{1}H NMR (CDCl$_3$, 400 MHz): δ 1.98-2.17 (m, 4H, CH$_2$), 3.61 (t, J = 6.7 Hz, 4H, CH$_2$), 7.58-7.68 (m, 1H, CH$_{Ar}$), 7.68-7.75 (m, 2H, CH$_{Ar}$), 7.85 (d, J = 7.8 Hz, 1H, CH$_{Ar}$). ^{13}C NMR (CDCl$_3$, 100 MHz): δ 25.5 (2CH$_2$), 48.4 (2CH$_2$), 107.5, 113.5, 122.6 (q, ^1J = 271.2 Hz), 125.4 (q, ^2J = 33.6 Hz), 127.4, 127.8 (q, ^3J = 5.2 Hz), 129.7, 132.8, 137.4, 156.0. Found: C, 54.9; H, 4.0; N 22.6%; C$_{14}$H$_{12}$F$_3$N$_5$ requires C, 54.7; H 3.9; N 22.8%. MS-EI m/z: 307 [M]$^+$.

2.2.13. (2-(4-Methoxyphenyl)-5-(pyrrolidin-1-yl)-2H-1,2,3-triazol-4-yl)(pyrrolidin-1-yl)methanone (4m). Colorless powder, yield: 297 mg (87%), mp 57-58 °C. FTIR, ν$_{max}$, cm^{-1}: 2970, 2865, 2836 (C-

8

H), 1613 (C=O). ^{1}H NMR (DMSO-d$_6$, 400 MHz): δ 1.87-2.05 (m, 8H, CH$_2$), 3.30-3.44 (m, 4H, CH$_2$), 3.48-3.60 (m, 2H, CH$_2$), 3.62-3.72 (m, 2H, CH$_2$), 3.83 (s, 3H, CH$_3$O), 6.98 and 7.81 (AA'XX', J = 8.8 Hz, 4H, CH$_{Ar}$). ^{13}C NMR (DMSO-d$_6$,100 MHz): δ 24.3 (CH$_2$), 25.4 (2CH$_2$), 26.3 (CH$_2$), 46.4 (CH$_2$), 48.4 (CH$_2$), 50.6 (2CH$_2$), 55.6 (CH$_3$O), 114.2 (2CH$_{Ar}$), 119.5 (2CH$_{Ar}$), 130.8, 133.6, 156.0, 158.5, 161.7 (C=O). Found: C, 63.5; H, 6.9; N 20.7%; C$_{18}$H$_{23}$N$_5$O$_2$ requires C, 63.3; H 6.8; N 20.5%. MS-EI m/z: 307. MS-EI m/z: 341 [M]$^+$.

2.2.14. Ethyl 2-(4-methoxyphenyl)-5-(pyrrolidin-1-yl)-2H-1,2,3-triazole-4-carboxylate (4n). Colorless powder, yield: 243 mg (77%), mp 85-86 °C. FTIR, ν$_{max}$, cm^{-1}: 2959, 2902, 2855 (C-H), 1703 (C=O). ^{1}H NMR (CDCl$_3$, 400 MHz): δ 1.45 (t, J = 7.1 Hz, 3H, C*H$_3$*CH$_2$O), 1.94-1.99 (m, 4H, CH$_2$), 3.47-3.52 (m, 4H, CH$_2$), 3.81 (s, 3H, CH$_3$O), 4.44 (q, J = 7.1 Hz, 2H, CH$_3$C*H$_2$*O) 7.11 and 7.85 (AA'XX', J = 9.3 Hz, 4H, CH$_{Ar}$). ^{13}C NMR (CDCl$_3$, 100 MHz): δ 14.4 (*CH$_3$*CH$_2$O), 25.6 (2CH$_2$), 50.4 (2CH$_2$), 55.6 (CH$_3$O), 61.0 (CH$_3$*CH$_2$*O), 114.2 (2CH$_{Ar}$), 120.3 (2CH$_{Ar}$), 128.2, 133.3, 155.6, 159.0, 161.7. Found: C, 61.0; H, 6.5; N 17.6%; C$_{16}$H$_{20}$N$_4$O$_3$ requires C, 60.8; H 6.4; N 17.7%. MS-EI m/z: 316 [M]$^+$.

2.2.15. (4-Chlorophenyl)(2-(4-methoxyphenyl)-5-(pyrrolidin-1-yl)-2H-1,2,3-triazol-4-yl)methanone (4o). Yellow powder, yield: 172 mg (45%), mp 89-90 °C. FTIR, ν$_{max}$, cm^{-1}: 2948, 2873, 2833 (C-H), 1650 (C=O). ^{1}H NMR (DMSO-d$_6$, 400 MHz): δ 1.91-2.08 (m, 4H, CH$_2$), 3.37-3.53 (m, 4H, CH$_2$), 3.85 (s, 3H, CH$_3$O), 7.02 and 7.88 (AA'XX', J = 9.0 Hz, 4H, CH$_{Ar}$), 7.55 and 8.08 (AA'XX', J = 8.5 Hz, 4H, CH$_{Ar}$). ^{13}C NMR (DMSO-d$_6$, 100 MHz): δ 25.1 (2CH$_2$), 49.8 (2CH$_2$), 55.5 (CH$_3$O), 114.7 (2CH$_{Ar}$), 119.9 (2CH$_{Ar}$), 128.4 (2CH$_{Ar}$), 131.8, 131.8 (2CH$_{Ar}$), 132.3, 136.4, 137.7, 155.2, 158.8, 184.0 (C=O). Found: C, 62.6; H, 5.1; N 14.5%; C$_{20}$H$_{19}$ClN$_4$O$_2$ requires C, 62.8; H 5.0; N 14.6%. MS-EI m/z: 382 [M]$^+$.

2.2.16. 2-(4-Methoxyphenyl)-5-(piperidin-1-yl)-2H-1,2,3-triazole-4-carbonitrile (4p). Colorless powder, yield: 243 mg (86%), mp 96-97 °C. FTIR, ν$_{max}$, cm^{-1}: 2990, 2978, 2940 (C-H), 2220 (CN). ^{1}H NMR (CDCl$_3$, 400 MHz): δ 1.62-1.89 (m, 6H, CH$_2$), 3.46-3.66 (m, 4H, CH$_2$), 3.88 (s, 3H, OCH$_3$), 6.98 and 7.91 (AA'XX', J = 9.1 Hz, 4H, CH$_{Ar}$). ^{13}C NMR (DMSO-d$_6$, 100 MHz): δ 24.0 (CH$_2$), 25.0

(2CH$_2$), 48.7 (2CH$_2$), 55.6 (CH$_3$O), 107.0, 114.4 (2CH$_{Ar}$), 120.3 (2CH$_{Ar}$), 132.9, 158.4, 159.5. Found: C, 63.8; H, 6.0; N 24.5%; C$_{15}$H$_{17}$N$_5$O requires C, 63.6; H 6.1; N 24.7%. MS-EI m/z: 283 [M]$^+$.

2.2.17. 2-(4-Methoxyphenyl)-5-morpholino-2H-1,2,3-triazole-4-carbonitrile (4q). Colorless powder, yield: 234 mg (82%), mp 128-129 °C. FTIR, ν_{max}, cm^{-1}: 2980, 2968, 2890, 2846 (C-H), 2221 (CN). ^{1}H NMR (CDCl$_3$, 400 MHz): δ 3.48-3.61 (m, 4H, CH$_2$), 3.80-3.93 (m, 7H, OCH$_3$ + CH$_2$), 6.99 and 7.91 (AA'XX', *J* = 9.1 Hz, 4H, CH$_{Ar}$). ^{13}C NMR (CDCl$_3$, 100 MHz): δ 47.7 (2CH$_2$), 55.6 (CH$_3$O), 66.1 (2CH$_2$), 107.1, 113.5 (CN), 114.4 (2CH$_{Ar}$), 120.3 (2CH$_{Ar}$), 132.7, 158.2, 159.7. Found: C, 59.1; H, 5.4; N 24.8%; C$_{14}$H$_{15}$N$_5$O$_2$ requires C, 58.9; H 5.3; N 24.6%. MS-EI m/z: 285 [M]$^+$.

2.2.18. 5-(Azepan-1-yl)-2-(4-methoxyphenyl)-2H-1,2,3-triazole-4-carbonitrile (4r). Colorless powder, yield: 255 mg (86%), mp 96-97 °C. FTIR, ν_{max}, cm^{-1}: 2976, 2952, 2890 (C-H), 2218 (CN). ^{1}H NMR (CDCl$_3$, 400 MHz): δ 1.55-1.68 (m, 4H, CH$_2$), 1.80-1.96 (m, 4H, CH$_2$), 3.62-3.72 (m, 4H, CH$_2$), 3.87 (s, 3H, CH$_3$O), 6.98 and 7.91 (AA'XX', *J* = 9.1 Hz, 4H, CH$_{Ar}$). ^{13}C NMR (CDCl$_3$, 100 MHz): δ 27.3 (2CH$_2$), 28.2 (2CH$_2$), 49.5 (2CH$_2$), 55.6 (CH$_3$O), 104.7, 114.3 (2CH$_{Ar}$), 114.5 (CN), 120.2 (2CH$_{Ar}$), 132.9, 157.0, 159.3. Found: C, 64.9; H, 6.3; N 23.7%; C$_{16}$H$_{19}$N$_5$O requires C, 64.6; H 6.4; N 23.6%. MS-EI m/z: 297 [M]$^+$.

2.2.19. 2-(4-Methoxyphenyl)-5-(4-(pyridin-2-yl)piperazin-1-yl)-2H-1,2,3-triazole-4-carbonitrile (4s). Colorless powder, yield: 202 mg (56%), mp 193-194 °C. FTIR, ν_{max}, cm^{-1}: 2982, 2946, 2880, 2840 (C-H), 2220 (CN). ^{1}H NMR (CDCl$_3$, 400 MHz): δ 3.62-3.78 (m, 8H, CH$_2$), 3.88 (s, 3H, CH$_3$O), 6.68-6.78 (m, 2H, CH$_{Pyr}$), 6.99 and 7.92 (AA'XX', *J* = 9.1 Hz, 4H, CH$_{Ar}$), 7.51-7.62 (m, 1H, CH$_{Pyr}$), 8.16-8.34 (m, 1H, CH$_{Pyr}$). ^{13}C NMR (CDCl$_3$, 100 MHz): δ 44.6 (2CH$_2$), 47.3 (2CH$_2$), 55.6 (CH$_3$O), 107.3, 107.4, 113.6, 114.0, 114.4 (2CH$_{Ar}$), 120.3 (2CH$_{Ar}$), 132.7, 137.7, 148.0, 158.1, 159.2, 159.7. Found: C, 62.8; H, 5.2; N 27.3%; C$_{19}$H$_{19}$N$_7$O requires C, 63.1; H 5.3; N 27.1%. MS-EI m/z: 361 [M]$^+$.

2.2.20. 5-([1,4'-Bipiperidin]-1'-yl)-2-(4-methoxyphenyl)-2H-1,2,3-triazole-4-carbonitrile (4t). Colorless powder, yield: 260 mg (71%), mp 249-250 °C. FTIR, ν_{max}, cm^{-1}: 2967, 2945, 2938, 2880 (C-H), 2220 (CN). ^{1}H NMR (CDCl$_3$, 400 MHz): δ 1.27-1.52 (m, 1H, CH$_2$), 1.81-2.03 (m, 5H, CH$_2$), 2.31-

10

2.59 (m, 4H, CH$_2$), 2.68-2.94 (m, 2H, CH$_2$), 3.06 (d, J = 12.4 Hz, 2H, CH$_2$), 3.15-3.68 (m, 3H, CH$_2$), 3.86 (s, 3H, CH$_3$O), 4.29 (d, J = 13.1 Hz, 2H, CH$_2$), 6.97 and 7.87 (AA'XX', J = 9.1 Hz, 4H, CH$_{Ar}$). ^{13}C NMR (CDCl$_3$, 100 MHz): δ 22.5, 22.7 (2CH$_2$), 25.2 (CH$_2$), 46.8 (2CH$_2$), 49.8 (2CH$_2$), 55.6 (CH$_3$O), 63.6, 107.3, 113.3, 114.5 (2CH$_{Ar}$), 120.3 (2CH$_{Ar}$), 132.5, 157.2, 159.8. Found: C, 65.4; H, 7.1; N 22.7%; C$_{20}$H$_{26}$N$_6$O requires C, 65.6; H 7.2; N 22.9%. MS-EI m/z: 366 [M]$^+$.

2.2.21. 5-(n-Butylamino)-2-(4-methoxyphenyl)-2H-1,2,3-triazole-4-carbonitrile ***(4u)****.* Colorless powder, yield: 163 mg (60%), mp 121-122 °C. FTIR, ν$_{max}$, cm^{-1}: 2992, 2938, 2880, 2858 (C-H), 2221 (CN). ^{1}H NMR (CDCl$_3$, 400 MHz): δ 1.00 (t, J = 7.4 Hz, 3H, CH$_3$), 1.46 (sext, J = 7.4 Hz, 2H, CH$_2$), 1.66 (quin, J = 7.4 Hz, 2H, CH$_2$), 3.42 (q, J = 7.4 Hz, 2H, CH$_2$), 3.87 (s, 3H, CH$_3$O), 4.17-4.29 (m,1H, NH), 6.98 and 7.90 (AA'XX', J = 8.8 Hz, 4H, CH$_{Ar}$). ^{13}C NMR (CDCl$_3$, 100 MHz): δ 13.8 (CH$_3$), 20.0 (CH$_2$), 31.7 (CH$_2$), 44.0 (CH$_2$), 55.6 (CH$_3$O), 106.4, 112.7, 114.4 (2CH$_{Ar}$), 120.2 (2CH$_{Ar}$), 132.9, 157.1, 159.4. Found: C, 62.3; H, 6.2; N 25.9%; C$_{14}$H$_{17}$N$_5$O requires C, 62.0; H 6.3; N 25.8%. MS-EI m/z: 271 [M]$^+$.

2.2.22. 5-(Cyclohexylamino)-2-(4-methoxyphenyl)-2H-1,2,3-triazole-4-carbonitrile ***(4v)****.* Colorless powder, yield: 180 mg (61%), mp 153-154 °C. FTIR, ν$_{max}$, cm^{-1}: 2930, 2850 (C-H), 2226 (CN). ^{1}H NMR (CDCl$_3$, 400 MHz): δ 1.20-1.34 (m, 3H, CH$_2$), 1.38-1.52 (m, 2H, CH$_2$), 1.61-1.75 (m, 1H, CH$_2$), 1.76-1.88 (m, 2H, CH$_2$), 2.08-2.18 (m, 2H, CH$_2$), 3.53-3.67 (m, 1H, CH), 4.10 (d, J = 7.7 Hz, 1H, NH), 6.99 and 7.90 (AA'XX', J = 9.1 Hz, 4H, CH$_{Ar}$). ^{13}C NMR (CDCl$_3$, 100 MHz): δ 24.7 (2CH$_2$), 25.6 (CH$_2$), 33.3 (2CH$_2$), 52.9 (CH), 55.6 (CH$_3$O), 106.9, 112.7, 114.4 (2CH$_{Ar}$), 120.2 (2CH$_{Ar}$), 132.9, 156.2, 159.4. Found: C, 64.9; H, 6.5; N 23.4%; C$_{16}$H$_{19}$N$_5$O requires C, 64.6; H 6.4; N 23.6%. MS-EI m/z: 297 [M]$^+$.

2.3. Electronic absorption and emission spectroscopy

UV-Vis absorption spectra were recorded on a Perkin-Elmer Lambda 35 UV-Vis spectrophotometer (Shelton, CT USA). Fluorescence of the sample solutions was measured using a

Hitachi F-7000 spectrophotometer (Tokyo, Japan). The absorption and emission spectra were recorded in MeCN, THF, $CHCl_3$, DMF, MeOH, EtOH and *n*-hexane using 10.00 mm quartz cells. The excitation wavelength was at the absorption maxima. Atmospheric oxygen contained in solutions was not removed. Concentration of the compounds in the solution was 1.0×10^{-5} M and 1.0×10^{-6} M for absorption and fluorescence measurements, respectively. The relative fluorescence quantum yields (Φ_F) were determined using quinine sulfate (1×10^{-5} M) in 0.1 M H_2SO_4 as a standard ($\Phi_F = 0.546$) [21].

2.4. X-ray crystallography

XRD data were obtained on an "Xcalibur S" diffractometer using a standard procedure (MoK-irradiation, graphite monochromator, ω-scanning with step 1°, T= 295(2) K). The structure was solved with the ShelXS structure solution program using Direct Methods and refined with the ShelXL refinement package using Least Squares minimization [22-24]. All non-hydrogen atoms were refined in anisotropic approximation, H-atoms were refined in isotropic approximation in the "riding" model.

Suitable single crystals of 1,2,3-triazoles **4d** and **4i** for X-ray structural analysis were obtained by slow evaporation of a solution of the compounds in chloroform at room temperature.

For **4d**, on the angles $3.00 < \Theta < 28.30^o$ 6542 reflections were measured, including 3233 unique ($R_{int} = 0.0300$) which were used in all calculations. Crystal data: $C_{14}H_{14}FN_5$, M = 271.30, monoclinic, $a = 19.5131(15)$ Å, $b = 16.2073(13)$ Å, $c = 8.7864(8)$ Å, $\beta = 99.370(7)$, V = 2741.7(4) Å^3, space group C2/c, Z = 8, μ(MoKα) = 0.093 mm^{-1}. The final $R^1 = 0.0991$, $wR^2 = 0.0742$ (all data) and $R^1 = 0.0360$, $wR^2 = 0.0684$ (I>2σ(I)), GooF= 1.007. Largest diff. peak and hole 0.133 and -0.106 ēÅ^{-3}.

For **4i**, on the angles $2.79 < \Theta < 26.37^o$ 5990 reflections were measured, including 2745 unique ($R_{int} = 0.0453$) which were used in all calculations. Crystal data: $C_{14}H_{15}N_5O$, M = 269.31, monoclinic, $a = 11.680(3)$ Å, $b = 8.7080(14)$ Å, $c = 13.742(3)$ Å, $\beta = 101.45(2)$, V = 1370.0(5) Å^3, space group P21/c, Z = 4, μ(MoKα) = 0.088 mm^{-1}. The final $R^1 = 0.1304$, $wR^2 = 0.1242$ (all data) and $R^1 = $

12

0.04940.0360, wR^2 = 0.1146 (I>2σ(I)), GooF= 1.002. Largest diff. peak and hole 0.237 and -0.188 ēÅ^{-3}.

A summary of the crystallographic data and structure refinement details are given in Supporting Information. The crystal structures of **4d** and **4i** are shown in Fig. 1. and Fig. 2.

CCDC 1472551 for compound **4d** and CCDC 1472552 for compound **4i** can be obtained free of charge from the Cambridge Crystallographic Data Centre via link www.ccdc.cam.ac.uk/data_request/cif.

2.5. Quantum Mechanical Calculations

The ground state molecular geometry of the compounds under investigation was fully optimized at Density Functional Theory (DFT) level, both *in vacuo* and in solvents (CH_2Cl_2 and MeCN). The harmonic vibrational frequencies and the thermochemicals were computed. We have compared the results obtained employing different functionals and different basis sets. In particular, we have chosen hybrid (*viz.* B3LYP [25], and M06−2X [26]) and long−range corrected (*viz.* CAM−B3LYP [27] and ωB97X [28]), coupled with the 6−31+G*, 6−311+G**, aug−cc−pVDZ and aug−cc−pVTZ [27-33] basis sets. Solvent effects were taken into account by means of the implicit Polarizable Continuum Model in its Integral Equation Formalism (IEF−PCM) [34]. The PCM molecular cavity was built according to the Universal Force Field (UFF) [35] radii, within the value used in the last implementation of the PCM (based on a continuum surface charge formalism). The standard values for the dielectric constants and refractive indexes were assumed. Both *in vacuo* and in solvents, the UV-Vis spectra were also simulated, accounting for $S_0 \rightarrow S_n$ (n = 1 to 5) transitions. The first $S(\pi,\pi^*)$ state geometry was subsequently optimized, using analytical gradients, and the first transitions $S_1 \rightarrow S_0$ of the emission transition. The Mulliken's charge population analysis and the electric dipole moment were also computed for the both ground and S_1 excited (vertical and relaxed) states. The calculations were performed using GAUSSIAN 09 [36].

3.   Results and discussion

3.1. Synthesis and characterization of 2-aryl-1,2,3-triazoles

The most important structural factors that influence fluorophore absorption and emission are the system conjugation, the direction and modulus of the electronic effects of the substituents and spatial effects, which may vary the conjugation on opposite parts of the molecule. To explore the relationship between these factors and the observed photophysical properties of 2-aryl-5-amino-1,2,3-triazoles, compounds **4a-v**, bearing various substituents within the aromatic ring and at positions 4 and 5 of the heterocycle (Scheme 1, Table 1) were synthesized. Compounds **4a-v** were produced using a recently reported one-pot reaction with the tandem addition of amines **2a-i** to arylhydrazononitriles **1a-o** and subsequent oxidative cyclization of intermediates **3** in the presence of copper(II) acetate (Scheme 1) [19]. This transformation typically proceeds in 1.5-7 h with moderate to good yields (60-92%). The longest conversion times were observed for the substrates **1n** and **1o**, where one of the CN-groups in the structure of hydrazone **1** was replaced with either an ethoxycarbonyl or aroyl group (Table 1, entries 14-15) and **4i-l** which bear one or two substituents in the *ortho*-position of the aryl moiety (Table 1, entries 9-12).

14
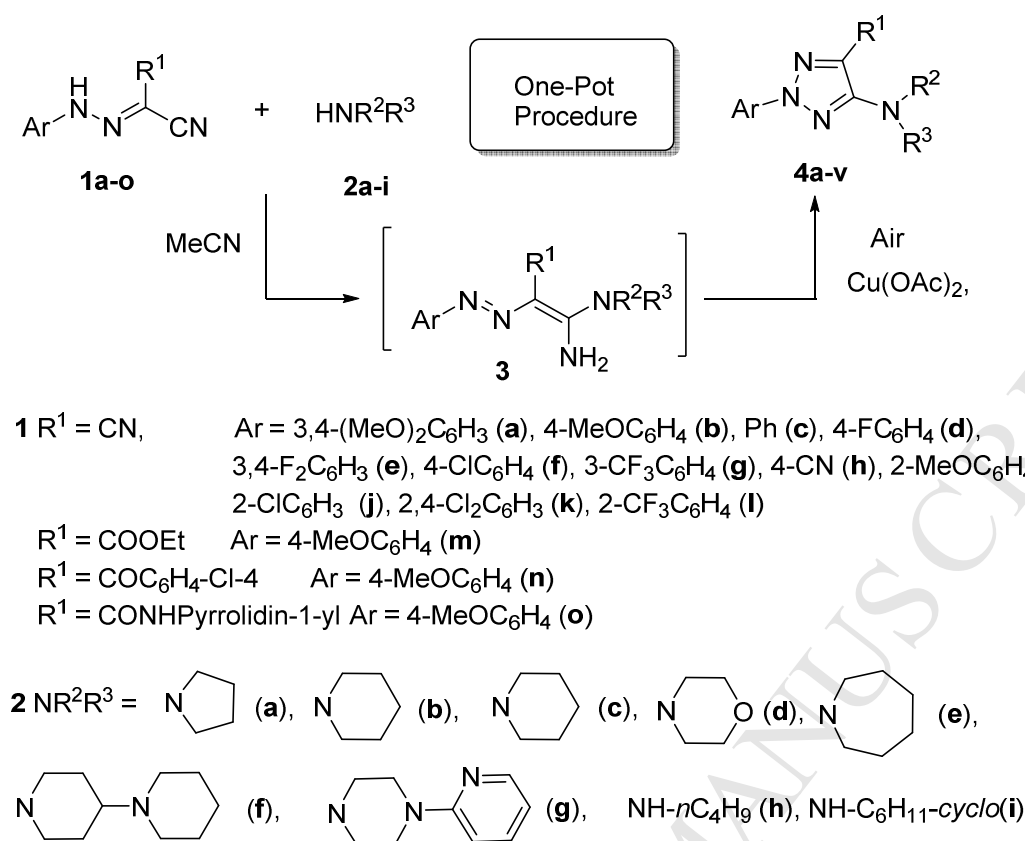
Scheme 1. One-pot synthesis of 2-aryl-1,2,3-triazoles **4a-v**.

Table 1

The time of conversion and yields for the one-pot synthesis of 2-aryl-1,2,3-triazoles **4a-v**

Entry	Triazole		Ar	NR^{2}R^3	Time (h)	Yield[a] (%)
	4	R^1				
1	**4a**	CN	3,4-(MeO)$_2$C$_6$H$_3$	Pyrrolidin-1-yl	6	87
2	**4b**	CN	4-MeOC$_6$H$_4$	Pyrrolidin-1-yl	2	92
3	**4c**	CN	C$_6$H$_4$	Pyrrolidin-1-yl	7	80
4	**4d**	CN	4-FC$_6$H$_4$	Pyrrolidin-1-yl	2	84
5	**4e**	CN	4-ClC$_6$H$_4$	Pyrrolidin-1-yl	3	84
6	**4f**	CN	3,5-F$_2$C$_6$H$_3$	Pyrrolidin-1-yl	7	90
7	**4g**	CN	3-CF$_3$C$_6$H$_4$	Pyrrolidin-1-yl	3	78

15

8	**4h**	CN	4-CNC$_6$H$_4$	Pyrrolidin-1-yl	15	73
9	**4i**	CN	2-MeOC$_6$H$_4$	Pyrrolidin-1-yl	11	78
10	**4j**	CN	2-ClC$_6$H$_4$	Pyrrolidin-1-yl	40	77
11	**4k**	CN	2,6-Cl$_2$C$_6$H$_3$	Pyrrolidin-1-yl	28	88
12	**4l**	CN	2-CF$_3$C$_6$H$_4$	Pyrrolidin-1-yl	50	80
13	**4m**	C(=O)Pyrrolidin-	4-MeOC$_6$H$_4$	Pyrrolidin-1-yl	4	87
14	**4n**	CO$_2$Et	4-MeOC$_6$H$_4$	Pyrrolidin-1-yl	20	77
15	**4o**	C(=O)C$_6$H$_4$Cl-4	4-MeOC$_6$H$_4$	Pyrrolidin-1-yl	24	45
16	**4p**	CN	4-MeOC$_6$H$_4$	Pyperidin-1-yl	3	86
17	**4q**	CN	4-MeOC$_6$H$_4$	Morpholin-4-yl	3	82
18	**4r**	CN	4-MeOC$_6$H$_4$	Azepane-1-yl	4	86
19	**4s**	CN	4-MeOC$_6$H$_4$	1-(2-Pyridyl) piperazine	5	56
20	**4t**	CN	4-MeOC$_6$H$_4$	1,4'-Bipiperidine	4	71
21	**4u**	CN	4-MeOC$_6$H$_4$	NH-n-C$_4$H$_9$	5	60
22	**4v**	CN	4-MeOC$_6$H$_4$	NHC$_6$H$_{11}$-$cyclo$	6	61

[a]Isolated yield (after the separation and purification).

The newly obtained 2H-1,2,3-triazoles **4a-v** were colorless solids. Their structure was confirmed by ^{1}H and ^{13}C spectroscopy, mass spectrometry and X-ray diffraction data for **4d,i** (Figs. 1 and 2).

3.2. X-ray crystallography analysis

The spatial structures of compounds **4d** and **4i** were determined by X-ray diffraction analysis (Figs. 1 and 2). According to the XRD data for triazole **4d**, atoms of CN- and Ph-groups are placed in the plane of the triazole ring (in limits of 0.025 Å). The piperidine group adopts a chair conformation with the heterocycle in the equatorial position. There are two hydrogen bonds between the C(10) and

16

C(14) hydrogen atoms in the *ortho*-positions of the aromatic ring and the N(3) and N(1) triazole atoms, respectively. In contrast, the aryl substituent in triazole **4i** is turned to the plane of triazole cycle at an angle of 53.7°.
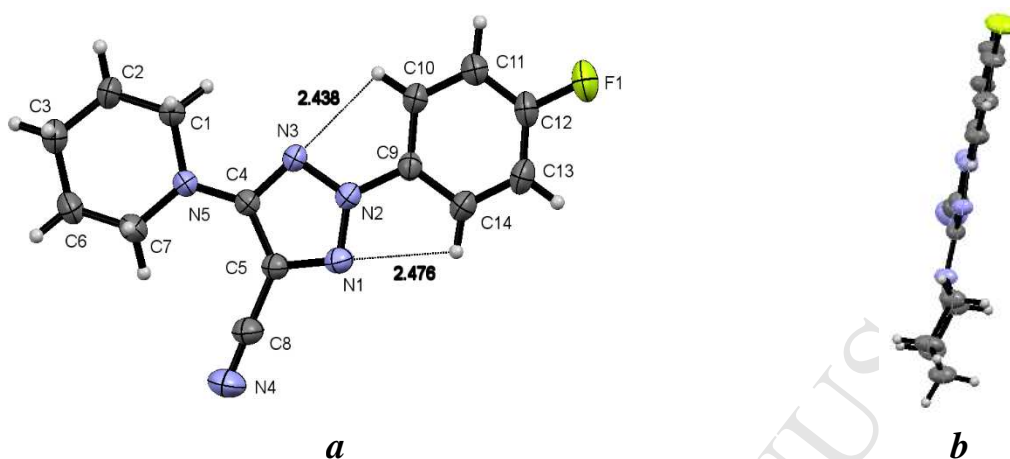
Fig. 1. ORTEP view of 1,2,3-triazole **4d** in thermal ellipsoids at 50% probability level: (*a*) front view and (b) side view. ($R_{WDW} = 2.7$Å).
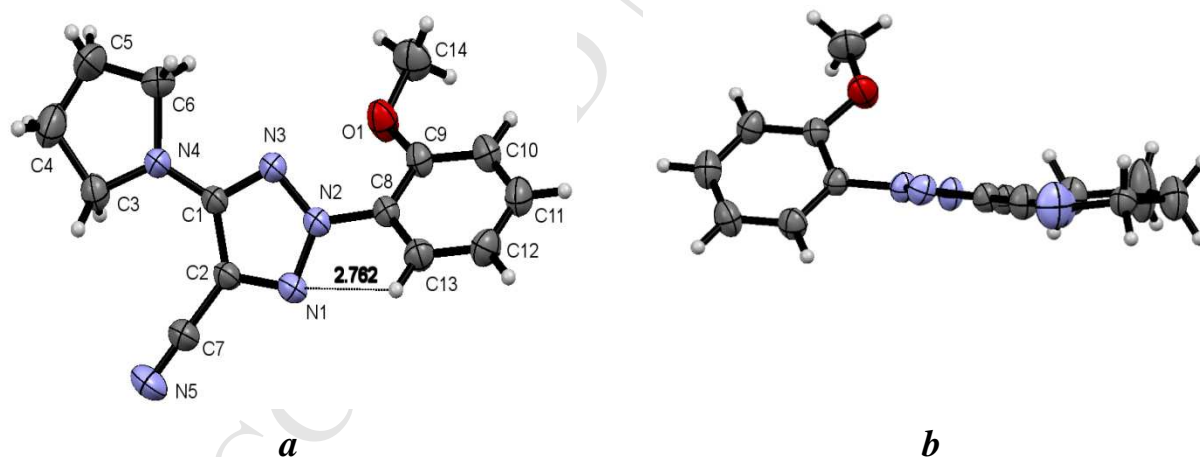
Fig. 2. ORTEP view of 1,2,3-triazole **4i** in thermal ellipsoids at 50% probability level: (*a*) front view and (*b*) side view.

Table 2.

Selected bond lengths for compounds **4d,i** according to XRD and the literature [37] data.

Entry	Literature data [37]	Compound **4d**	Compound **4i**

	Bond length, Å	Bond	Bond length, Å	Bond	Bond length, Å
1	1.366	N(1)-N(2)	1.3143(14)	N(2)-N(1)	1.311(2)
2	1.366	N(2)-N(3)	1.3517(12)	N(2)-N(3)	1.338(2)
3	1.329	N(1)=C(5)	1.3399(16)	C(2)=N(1)	1.337(3)
4	1.329	N(3)=C(4)	1.3405(15)	N(3)=C(1)	1.329(3)
5	1.431	N(2)-C(9)	1.4237(16)	N(2)-C(8)	1.423(3)
6	1.416	C(4)-N(5)	1.3638(15)	N(4)-C(1)	1.336(3)
7	1.136	N(4)≡C(8)	1.1400(18)	C(7)≡N(5)	1.131(3)
8	1.444	C(5)-C(8)	1.422(2)	C(2)-C(7)	1.408(4)

Analysis of the bond lengths for the compounds **4d** and **4i** (Table 2) reveals the shortening of the single bond lengths and elongation of the double and triple bonds caused by conjugation within the molecule core.

3.3. Optical properties of 2-aryl-1,2,3-triazoles
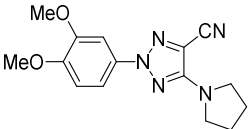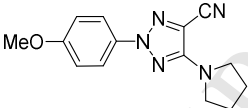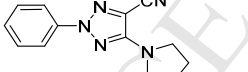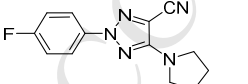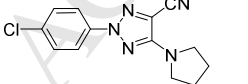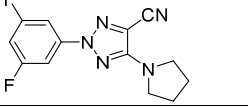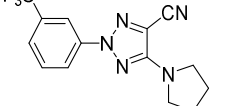
2-Aryl-5-amino-1,2,3-triazoles **4a-v** dissolve in most common organic solvents including MeCN, THF, CHCl$_3$, DMF and DMSO. The photophysical properties of compounds **4a-v** were examined by UV-Vis and fluorescence spectroscopy in acetonitrile at room temperature and the results are summarized in Table 3. All of the investigated compounds exhibited similar absorption and emission contours (Figs 4, 6, 8-10). The absorption spectra for compounds **4** showed two strong maxima at approximately 229-259 nm and 317-381 nm. The emission spectra of solutions of 2-aryl-1,2,3-triazoles **4a-v** were measured at an excitation wavelength corresponding to the long-wavelength maximum in the absorption spectra. Typical emission maxima obtained upon irradiation of the
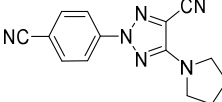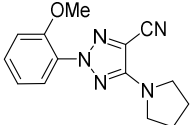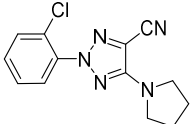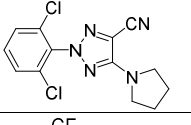
18
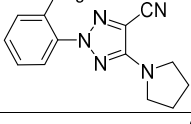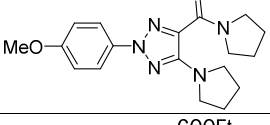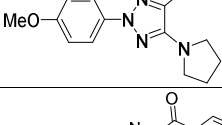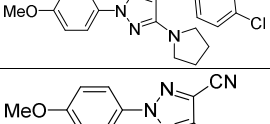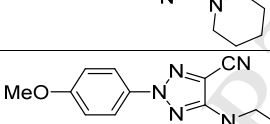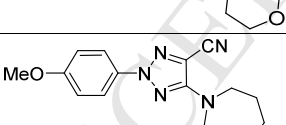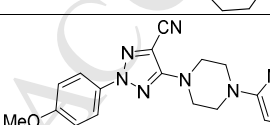
solutions were in the blue region. Interestingly, many of the compounds exhibited a significant Stokes shift up to 140 nm (9461 cm^{-1})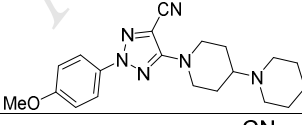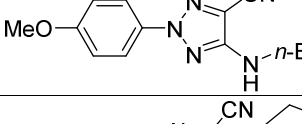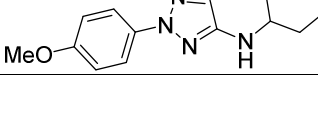, although the extent of the shift varied significantly between structures. Spectral characteristics such as absorption (λ_{abs}), emission (λ_{em}), molar absorption coefficient (ε) and quantum yield (Φ_F) for the compounds **4a-v** were measured in acetonitrile and are presented in Table 3.

As follows from the spectral characteristics (Stokes shift and quantum yield), most of compounds **4a-v** have exhibited a strong fluorescence.

Table 3

Photophysical data for 2-aryl-1,2,3-triazoles **4** (solution in acetonitrile).

Entry	Triazole		UV-Vis		Fluorescence		Stokes shift, (nm/cm^{-1})
	4	Structure	λ_{abs} (nm)	lgε_{max}	λ_{em} (nm)	Φ_F	
1	**4a**		240 344	4.22 4.08	417	0.996	73/6115
2	**4b**		247 340	4.43 4.13	418	0.936	78/5488
3	**4c**		243 340	4.50 4.05	423	0.886	83/5771
4	**4d**		243 340	4.28 3.85	422	0.683	82/5715
5	**4e**		251 346	4.37 3.86	429	0.829	83/5592
6	**4f**		245 350	4.27 4.11	435	0.837	85/5583
7	**4g**		247 347	4.27 4.04	430	0.801	83/5563

19

8	**4h**		259 362	4.41 4.19	446	0.579	84/5202
9	**4i**		240 318	3.89 3.81	418	0.456	100/7523
10	**4j**		229 324	4.11 3.73	426	0.607	102/7309
11	**4k**		238 317	3.08 3.69	418	0.113	101/7622
12	**4l**		227 326	4.17 3.79	433	0.710	107/7580
13	**4m**		250 328	3.98 3.99	412	0.555	84/6216
14	**4n**		256 336	4.26 4.06	423	0.731	87/6121
15	**4o**		266 381	4.33 4.01	421	0.004	40/2494
16	**4p**		239 340	4.16 4.08	415	0.929	84/6115
17	**4q**		245 324	4.14 4.14	410	0.856	86/6474
18	**4r**		250 344	4.29 4.13	413	0.980	69/4857
19	**4s**		250 321	4.48 4.14	461	0.064	140/9461
20	**4t**		247 325	3.97 4.12	403	0.156	78/5955
21	**4u**		240 328	4.11 4.19	401	0.918	73/5550
22	**4v**		241 330	4.16 4.20	402	0.956	72/5427

[a]UV-Vis absorption wavelengths at room temperature and concentration 10^{-5} M.

[b]Fluorescence wavelengths at room temperature and concentration 10^{-6} M.

[c]Fluorescence quantum yields measured using a 0.1 M H_2SO_4 solution of quinine sulfate ($\Phi_F = 0.55$) as a reference.

3.3.1 Structure and optical properties

The spectral properties of compounds **4a-v** depend on their electronic structure. These properties are influenced by the conjugation of the aromatic and triazole rings, the nature of substituents within aromatic cycle, the type of amino group at C(5) position of triazole and the type of electron-withdrawing group (R^1 = CN, $CONR^2R^3$ or $C(=O)C_6H_4Cl$-4) at C(4) of triazole ring. To rationalize the relationship between the structure of investigated compounds and their photophysical properties, we have divided them into several groups in accordance with the above-mentioned structural features.

The XRD (Fig. 1) and computational data (Table 4, Supporting Information, Table S2) for triazoles **4a-h** shows the planar molecular construction of these compounds, which provides good conjugation between opposite fragments of the molecule. Thus, triazoles **4a-h** were considered a suitable model to establish the relationship between the electronic effects of substitutions on the aryl moiety and the emission and absorption properties.

Analysis of absorption and emission spectral data for triazoles **4a-h** revealed that the presence of strong electron-withdrawing groups within aromatic ring (compound **4h**) leads to a red-shift (up to 22 nm/1787 cm^{-1}) in its absorption spectrum and a 29 nm/1559 cm^{-1} red-shift in the emission spectrum (Table 3, Fig. 4). Thus, the most effective conjugation is observed when a CN group in the aryl and triazole C(5)-amino group are both present (as in triazole **4h**). In contrast, the quantum yield is highly dependent on the degree of conjugation, and it decreases from 0.996 for compound **4a** (Ar = 3,4-$(MeO)_2C_6H_3$) to 0.579 for compound **4h** (R^1 = CN) (Table 3). Therefore, the strong fluorescence of **4a**

21

and **4b** is likely caused by better internal charge transfer (ICT) from the electron-donating OMe to the electron-withdrawing $C(4)_{triazole}$-CN upon light excitation.

Fig. 3 (*a*) Photographs of the solutions of **4a-h** under irradiation with hand-held UV lamp at emission wavelength of 380 nm. (*b*) Photographs of the same solutions taken under daylight.
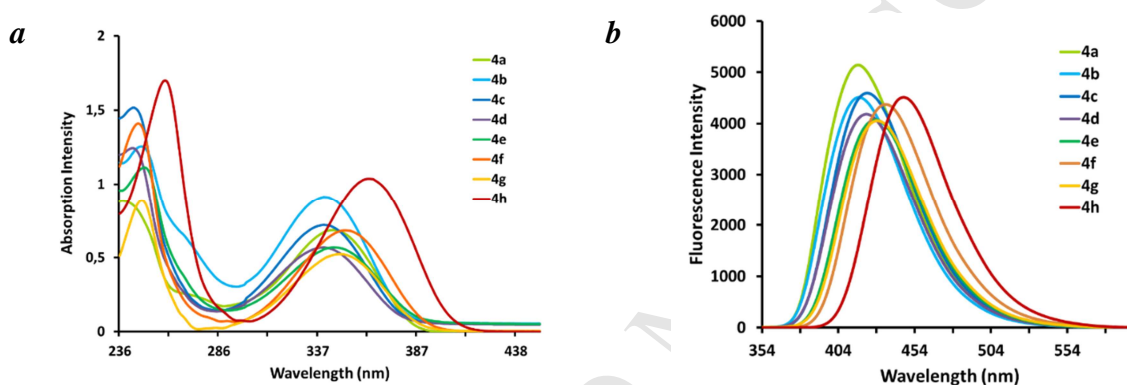

Fig. 4. Absorption (*a*) and emission (*b*) spectra of 2-aryl-1,2,3-triazoles **4a-h** in MeCN at room temperature.

Triazoles **4i-l** contain either one or two substituents at the *ortho*-position of aromatic ring and can be used to establish the influence of steric hindrance on the photophysical properties of the compounds (Table 3, entries 9-12, Figs. 5, 6). The XRD results and the data calculated for the ground states (Fig. 2, Table 6 and Supporting Information, Table S2) for these molecules indicates that the conjugation between the aromatic and heterocyclic ring systems is disrupted. The strongest intramolecular repulsion occurs in **4i-l** and leads to a significantly twisted molecular conformation. Triazoles **4i-l** showed blue shifts up to 33 nm/2974 cm^{-1} in the absorption spectra coupled with a decrease in the molar adsorption coefficient (Table 3, entries 9-12), but the emission parameters were nearly identical to the compounds with *para*-located substituents. These spectral features of compounds **4i-l** afforded

an increase in the Stokes shifts (up to 107 nm/7580 cm^{-1} for **4l**) and a decrease in the quantum yields (0.113-0.71). These results suggest a twisted intramolecular charge transfer (TICT) is realized for triazoles **4i-l** as opposed to planar compounds **4a-h**.
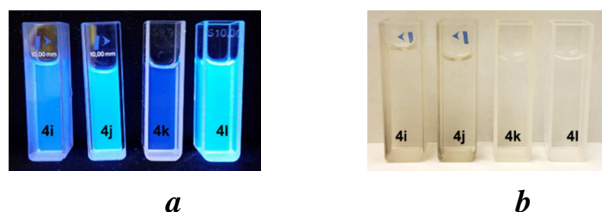

a   *b*

Fig. 5. (*a*) Photographs of the solutions in MeCN of **4i-l** under irradiation with hand-held UV lamp at emission wavelength of 380 nm. (*b*) Photographs of the same solutions taken under daylight.
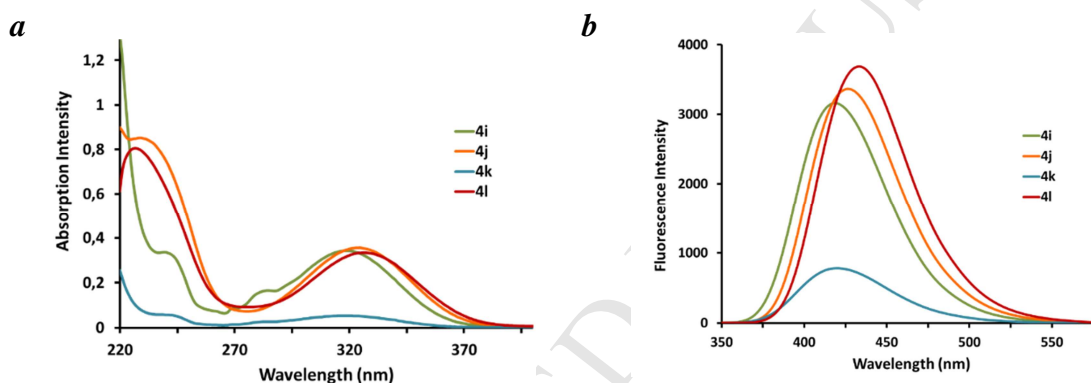

Fig. 6. Absorption (*a*) and emission (*b*) spectra of 2-aryl-1,2,3-triazoles **4i-l** in MeCN at room temperature.

The experimental data for triazoles **4b** and **4p-v** confirm that the type of alkylamino group at C(5) of the heterocycle has a dramatic effect on both the Stokes shift and the quantum yield (Table 3, entries 2, 16-22, Figs. 7, 8). For example, the replacement of the azepane moiety (compound **4r**) by 4-(pyridin-2-yl)piperazine fragment (compound **4s**) caused an apparent blue-shift of the absorption maximum from 344 to 321 nm, an increase in the Stokes shift from 69 nm (4857 cm^{-1}) to 140 nm (9461 cm^{-1}) and a substantial decrease in the quantum yield (to 0.064). The relatively low quantum yields observed for compounds **4s** and **4t** imply a strong non-radiative deactivation pathway for their excited states.
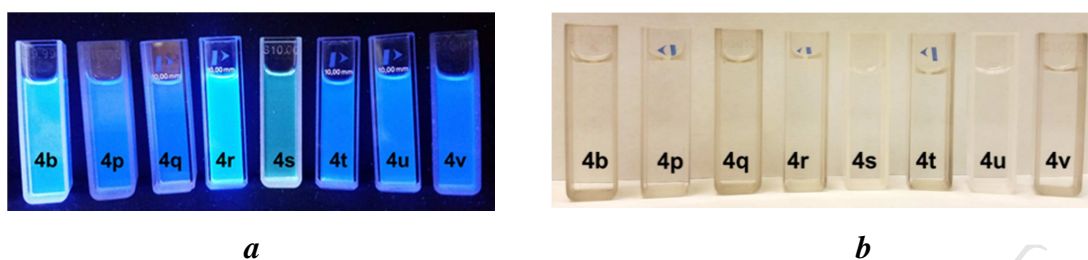
a   *b*

Fig. 7. (*a*) Photographs of the MeCN solutions of **4b**, **p-v** under irradiation with hand-held UV lamp at emission wavelength of 380 nm. (*b*) Photographs of the same solutions taken under daylight at room temperature.
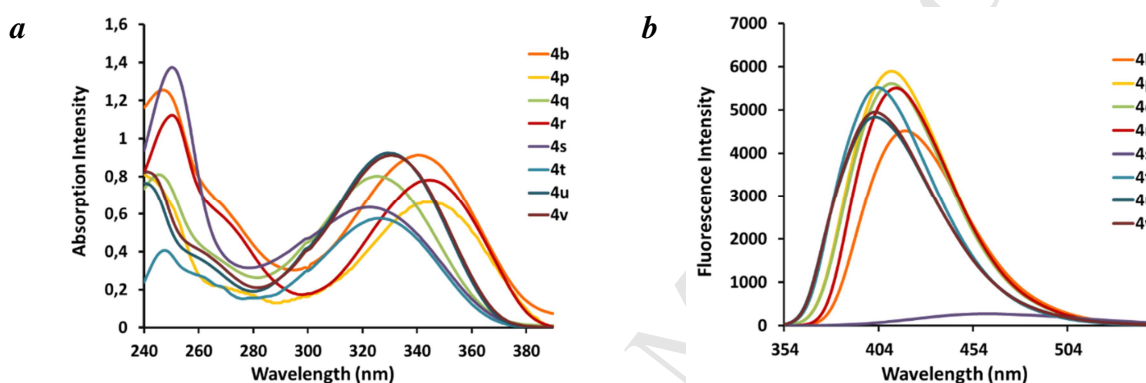

Fig. 8. Absorption (*a*) and emission (*b*) spectra of 2-aryl-1,2,3-triazoles **4b**,**p-v** in MeCN at room temperature.

The last group of investigated compounds, **4b** and **4m-o**, differ in substitution only at the triazole C(4) position. Absorption spectra of these triazoles exhibited increasing red-shifts in the order **4m** < **4n** < **4b** < **4o** (Table 3, Figs. 9, 10). Further, replacement of the CN-moiety in the molecule of triazole **4b** by any other function led to unfavourable emission parameters. While compound **4b** exhibited extremely high fluorescent emission with a quantum yield >0.90, compound **4o** showed very weak blue emission with a fluorescence quantum yield of 0.004 and a maximum emission wavelength of 421 nm when excited at 381 nm (Table 3, entry 15).
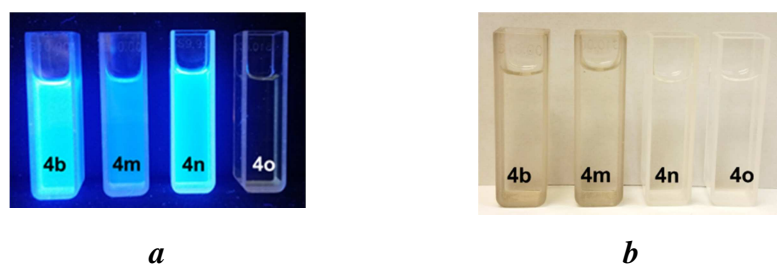
Fig. 9. (*a*) Photographs of the solutions in MeCN of **4b,m,n,o** under irradiation with hand-held UV lamp at emission wavelength of 380 nm. (*b*) Photographs of the same solutions under daylight.
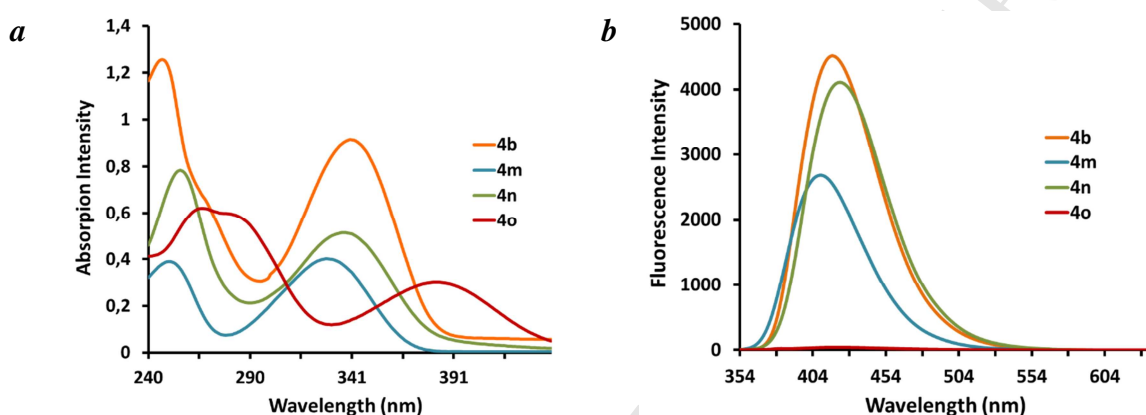

Fig. 10. Absorption (*a*) and emission (*b*) spectra of 2-aryl-1,2,3-triazoles **4b,m,n,o** in MeCN at room temperature.

The observed photophysical phenomena reveal that the optical properties of the investigated triazoles **4a-v** are very sensitive to structural factors, which allows one to readily tune the photophysical properties of the fluorophores by appropriate design of the molecule. Among all of the products studied, compound **4a** showed the highest quantum yield (0.996) and a moderate Stokes shift (73 nm/6115 cm^{-1}), whereas triazole **4s** exhibited the largest Stokes shift and one of the lowest quantum yield (0.064) (Table. 3, entry 19). It is worth nothing that quantum yields of most of the triazoles investigated were better than for previously investigated 1*H*-triazoles and even for known examples of 2*H*-triazole derivatives [11-18].

3.3.2 Solvatochromism

25

Among the major environmental factors influencing electronic spectra, solvent effects are of particular importance. Solvatochromism involves a change in the absorption and emission spectra and/or quantum yields when the fluorophore is dissolved in solvents of different polarity. The solvatochromic effect of compounds **4** was investigated to estimate the difference between the dipole moment for the ground states and excited states of these molecules. The absorption and emission spectra of compounds **4b**, **4m** and **4v** were recorded at a standard concentration in different solvents with varying polarity, including acetonitrile, chloroform, DMF, ethanol, methanol and *n*-hexane (Table 4, Figs. 12-14).

Fig. 11. (*a*) Photographs of the solutions of **4b** under irradiation with hand-held UV lamp at emission wavelength of 380 nm. (*b*) Photographs of the same solutions under daylight.
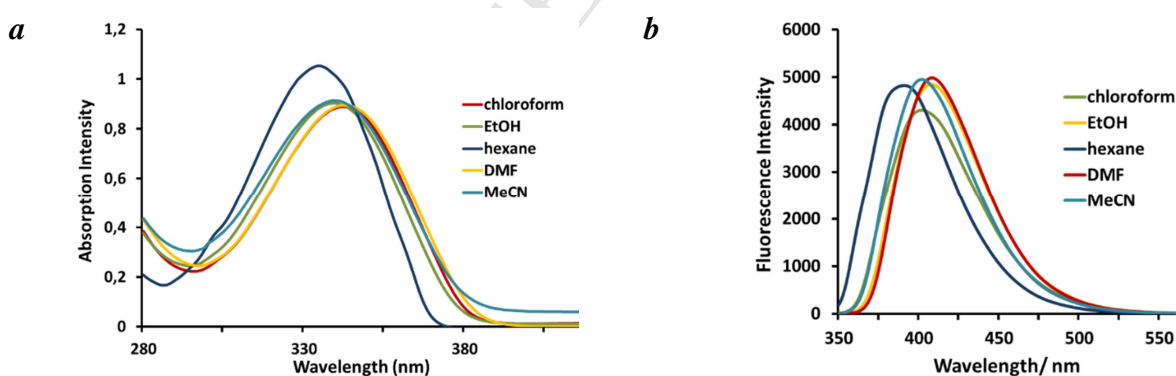

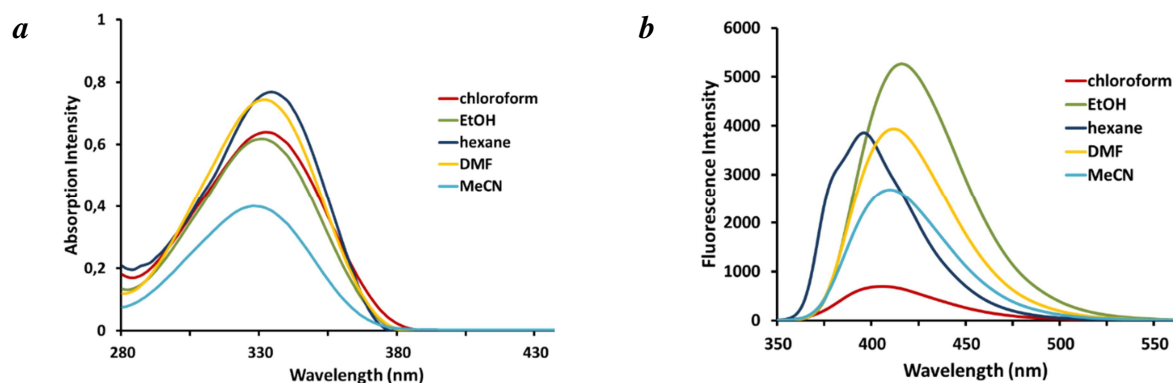**Fig. 12.** Absorption (*a*) and emission (*b*) spectra of 1,2,3-triazoles **4b** in different solvents at 25 °C.

Fig. 13. Absorption (*a*) and emission (*b*) spectra of 1,2,3-triazole **4m** in different solvents at 25 °C.
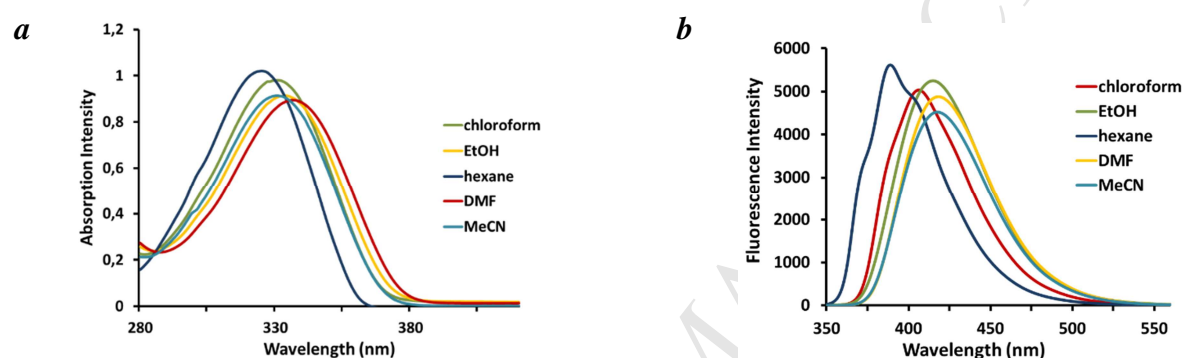

Fig. 14. Absorption (*a*) and emission (*b*) spectra of 2-aryl-1,2,3-triazoles **4v** in different solvents at 25 °C.

Table 4

Fluorescence characteristics of 2-aryl-1,2,3-triazoles **4b,m,v** in organic solvents

Entry	Compound	Solvent	f (ε,n^2)[a]	λ_{abs}, (nm)	lgε	λ_{em} (nm)	Stokes shift (nm/cm^{-1})	Φ_F
1	**4b**	*n*-Hexane	-0.001	335	4.21	389(	54/4143	-[b]
2		CHCl$_3$	0.149	342	4.17	406	64/4609	-[b]
3		DMF	0.275	343	4.14	418	75/5520	-[b]
4	MeO⟨...⟩	EtOH	0.290	339	4.18	415	76/5402	-[b]
5		MeOH	0.309	340	4.17	416	76/5373	0.98
6		MeCN	0.305	340	4.13	418	75/5488	0.94
7	**4m**	*n*-Hexane	-0.001	332	4.13	405	73/5429	0.64
8		CHCl$_3$	0.275	331	4.17	411	80/5880	0.77
9		DMF	0.290	334	4.18	396	62/4687	0.90
10		EtOH	0.305	328	3.99	410	82/6097	0.55
11		MeCN	0.149	332	4.13	405	73/5429	0.11
12	**4v**	*n*-Hexane	-0.001	325	4.23	391	66/5193	-[b]
13	MeO⟨...⟩	CHCl$_3$	0.149	330	4.21	402	72/5427	-[b]

14	DMF	0.275	336	4.17	408	72/5252	-[b]
15	EtOH	0.290	333	4.20	408	75/5520	-[b]
16	MeCN	0.305	330	4.20	402	72/5427	0.95

[a] The polarity scale chosen is the orientation polarizability employed in the Lippert-Mataga equation $f(\varepsilon, n^2) = [(\varepsilon-1)/(2\varepsilon-1)]-[(n^2-1)(2n^2+1)]$, taking into account both the solvent dielectric constant and refractive index [1].

[b] Not detected.

The UV spectra of **4b**, **4m** and **4v** were essentially unchanged in all of the solvents examined, implying a weak positive solvent-dependence (Table 4, Figs. 12-14). In contrast, the maximum emission wavelength for these compounds showed a slight bathochromic shift in more polar solvents, as illustrated in Figs. 12-14. As shown in Table 4, compound **4m** is most affected by the solvent polarity, exhibiting a bathochromically shifted emission maximum in polar solvents (ethanol, methanol and DMF) compared to non-polar *n*-hexane. The Stokes shift for compounds **4b** and **4m** vary widely in different solvent (1193 and 1259 cm^{-1}), while the Stokes shift for compound **4v** shows very little solvent influence (327 cm^{-1}). These effects are explained by a slight increase in the dipole moment of the excited states (see Table 5), leading to increased sensitivity toward the surrounding environment. The intensity of absorption and emission for triazole **4m** is also highly dependent on solvent polarity. In particular, the quantum yield of triazole **4m** decreases drastically with decreasing polarity of the solvents (EtOH [0.90] > DMF [0.77] > *n*-hexane [0.64] > MeCN [0.55] > CHCl$_3$ [0.11]). The highest fluorescence quantum yield was observed in ethanol, a polar, protic solvent. It is possible that the triazole **4m** with the carboxamide group at C(4) atom of heterocyclic ring is more readily able to form hydrogen bonds with the alcoholic solvent than the other proton-donor compounds. This is a very important interaction (along with the dipole-dipole interactions) that significantly affects the quantum yield. It should be mentioned that the quantum yield of all of the investigated compounds increased

substantially in alcoholic solvents. Even triazole **4b**, which had an excellent quantum yield in acetonitrile (0.93), was further improved in methanol (0.98).

It is known that specific solvent–fluorophore interactions could occur either in the ground or in the excited states [1,2]. As for the investigated triazoles **4**, the influence of the solvents appears to have a larger effect on the emission spectrum than on the absorption spectrum, which suggests that dipolar moment of the excited states is higher than that in ground state. This statement is supported by the results from theoretical calculations (Table 5).

3.3. Quantum Mechanical Calculations

The absorption (λ_{abs}) and emission (λ_{em}) wavelength and oscillator strength ($f_{01,} f_{10}$), Stokes shifts (Δv), the modulus of the electric dipole moments of the ground state (μ_0), of the vertical FC excited (μ_{1v}) and of the relaxed excited states (μ_{1r}) and the angles formed by the dipole moment vectors ($\theta_{0,1v}$ and $\theta_{0,1r}$) were computed at the DFT CAM-B3LYP/cc-pVTZ level of theory, in the implicit solvated phase (MeCN). The data provided in Table 5 are in excellent agreement with the experimental spectroscopic measurements (Table 3), and the calculated oscillator strength for the absorption transition changes is in accordance with experimental absorption and emission characteristics.

Table 5

Computed absorption wavelength (λ_a) and oscillator strength (f_{01}), emission wavelength (λ_e) and oscillator strength (f_{10}), Stokes shift (Δv), the modulus of the electric dipole moment of the ground state (μ_0), of the vertical FC excited (μ_{1v}) and of the relaxed excited states (μ_{1r}) and the angles formed by the dipole moment vectors ($\theta_{0,1v}$ and $\theta_{0,1r}$) for triazoles **4a-v**.

Compound	λ_{abs} (nm)	f_{01}	λ_{em} (nm)	f_{10}	$\Delta v / k_K$	μ_0 (D)	μ_{1v} (D)	μ_{1r} (D)	$\theta_{0,1v}$ (°)	$\theta_{0,1r}$ (°)
4a	345	0.4084	416	0.7881	4.952	6.79	10.79	6.56	23	4
4b	339	0.3778	417	0.7431	5.523	8.54	12.41	8.23	25	3
4c	340	0.2705	421	0.5817	5.664	6.43	12.04	6.10	39	8
4d	341	0.2680	420	0.5692	5.521	6.19	13.02	6.20	26	7
4e	347	0.3095	427	0.6484	5.404	6.21	13.51	6.28	27	8

4f	349	0.2621	433	0.5417	5.564	6.23	14.18	6.39	26	9
4g	348	0.2712	431	0.5631	5.539	9.38	16.53	9.31	25	5
4h	363	0.3771	444	0.7530	5.030	8.03	19.27	8.79	15	6
4i	318	0.1649	416	0.6690	7.415	6.91	11.31	5.39	42	28
4j	325	0.1649	424	0.5541	7.191	7.95	13.28	8.04	39	12
4k	317	0.1306	417	0.3850	7.572	7.39	12.36	6.56	34	15
4l	327	0.1883	434	0.5833	7.547	9.26	14.92	9.63	46	14
4m	327	0.4561	410	0.7211	6.197	5.20	7.17	4.26	49	3
4n	335	0.3714	421	0.6552	6.103	3.28	7.95	3.20	41	19
4o	383	0.2871	422	0.0498	2.415	6.08	16.34	5.54	15	54
4p	332	0.4406	416	0.7093	6.088	8.47	11.80	8.29	16	9
4q	325	0.5204	408	0.7604	6.265	7.90	11.14	7.67	6	6
4r	347	0.3738	411	0.7261	4.492	8.51	12.11	8.20	24	4
4s	320	0.5417	460	0.7620	9.520	10.31	13.74	10.17	3	5
4t	326	0.4719	401	0.7279	5.743	8.59	11.86	8.29	12	9
4u	329	0.3597	400	0.8070	5.400	8.09	10.81	7.84	27	10
4v	331	0.5186	402	0.7899	5.341	8.48	11.88	8.06	3	4

Ground state and excited state dipole moments had values ranging from 3.28 to 10.31D and from 7.17 to 19.27D, respectively (Table 5). The changes in the dipole moment of the triazoles (particularly **4h** and **4o**) and the angles formed by the dipole moment vectors ($\theta_{0,1v}$) indicated that the polarity of these compounds changes significantly during the transition to the excited state. The increase in the excited state electric dipole moment (μ_{1v}), compared with the dipole moment of the ground state (μ_0), is caused by solvent-solute interactions that stabilize the excited electronic state in polar solvents (positive solvatochromic effect). The computational data confirmed the solvent effects discussed previously (see section 3.3.2). The higher excited state dipole moment also indicates a redistribution of charge densities between the ground and excited states. Furthermore, the charge transfer process occurs in the excited state rather than in ground state. The emission process and the transient relaxed excited state effectively reduce the polarity parameters of the molecules back to their ground state values because the modulus of the electric dipole moment of the ground state (μ_0) and the relaxed excited state (μ_{1r}) are very close, as are the angles formed by the dipole moment vectors ($\theta_{0,1r}$).

The molecular structures predicted at the DFT level were in good agreement with the experimental results (part 3.2). The calculations revealed that aryl substituents located at the 2-position of the triazole ring for compounds **4a-h** and **4i-e** are coplanar, as seen in the X-ray data (Table 2, Fig. 2). The major geometric changes upon excitation, presented in Table 6, are associated with the length of the C-

N bond and the torsions between the two rings. As expected, the conjugation between the triazole and the aromatic ring increases sharply in the excited state. The length of the C-N bond linking these two cycles and the torsion angle between them indicate a dramatic increase in planarity of the molecular structure of **4a-h** and **4i-e** upon excitation. Compounds **4i**, **4j** and **4l** showed the most substantial changes in torsion angles in the relaxed excited state and, coincidentally, provided better emission parameters than would be expected based on their structures (Figs. 1 and 2, Tables 2 and 6). Even for triazole **4k**, which bears two chlorine atoms at the *ortho*-positions of the aromatic ring, the calculations predict a large change in the torsional angle between the two cycles (from 90.7° in ground state to 45° in the excited state) and a decrease in the C-N bond length of 0.048 Å (Table 6, entry 11).
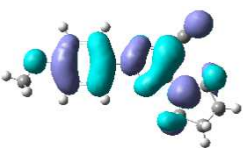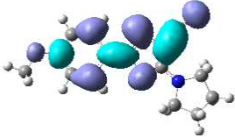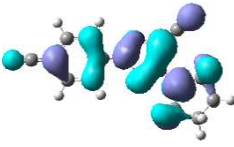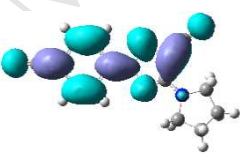
Table 6
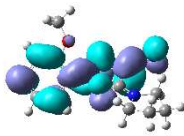
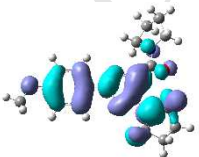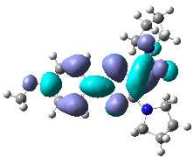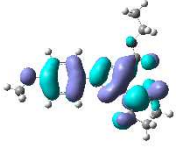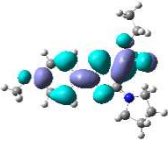Bond length (*b*) and dihedral angle (δ) between the aromatic and triazole rings for the ground (S_0) and the excited states (S_1) relaxed geometries of triazoles **4a-v** in MeCN.

Entry	Triazole	$b(S_0)$ (Å)	$\delta(S_0)$ (°)	$b(S_1)$ (Å)	$\delta(S_1)$ (°)
1	**4a**	1.425	1.6	1.351	0.1
2	**4b**	1.425	1.1	1.352	0.0
3	**4c**	1.425	0.6	1.359	0.1
4	**4d**	1.424	1.1	1.359	0.1
5	**4e**	1.422	0.6	1.358	0.1
6	**4f**	1.418	0.6	1.360	0.1
7	**4g**	1.421	0.2	1.361	0.2
8	**4h**	1.416	0.4	1.359	0.1
9	**4i**	1.431	66.4	1.359	19.9
10	**4j**	1.427	60.8	1.366	22.3
11	**4k**	1.425	90.7	1.377	45.0
12	**4l**	1.429	55.3	1.367	14.5
13	**4m**	1.421	3.7	1.354	0.7
14	**4n**	1.424	4.0	1.358	0.2
15	**4o**	1.424	2.4	1.412	1.9
16	**4p**	1.426	4.4	1.353	0.1
17	**4q**	1.426	3.8	1.350	0.1
18	**4r**	1.425	2.4	1.352	0.2
19	**4s**	1.426	4.4	1.350	0.1
20	**4t**	1.426	3.5	1.352	0.1
21	**4u**	1.426	2.1	1.347	0.2
22	**4v**	1.425	0.3	1.347	0.1

To visualize the charge delocalization, we have plotted the frontier molecular orbitals of the representative compounds **4b**, **4h**, **4i**, **4m**, **4n**, **4o** and **4s** (Fig. 15). For compounds **4b**, **4h** and **4i**, the

31

electronic distribution of the HOMO is spread throughout the whole molecule, whereas the LUMO electronic distribution excludes the *tert*-alkylamino group. This difference provides better overlap of the HOMO and LUMO and promotes a large transition moment of the $S_1 \rightarrow S_0$ transitions for triazoles **4b**, **4h, 4i**, **4m** and **4n**. In contrast, compounds **4o** and **4s** have electronic distributions in the ground state and excited states that are quite different.

The HOMO and LUMO of the triazole derivatives bearing cyano (**4b**, **4h, 4i**), carboxamide (**4m**) and ethoxycarbonyl (**4n**) substituents at the C(5) triazole atom are similar, but the strong influence of the electron deficient aryl substituent in compound **4o** effectively modifies the LUMO distribution.
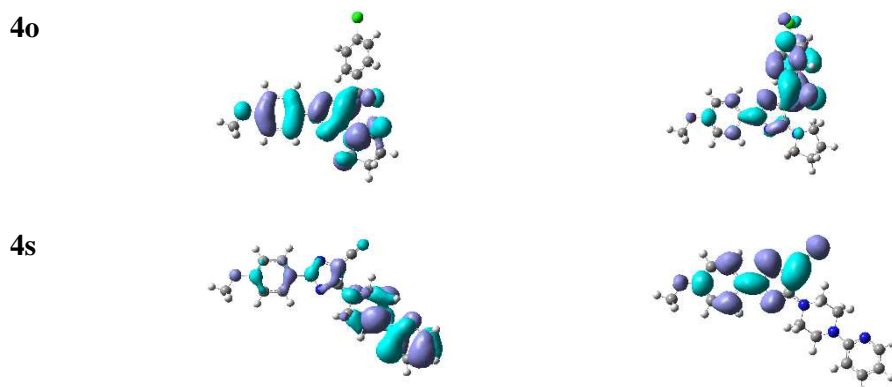
Compound	HOMO	LUMO
4b		
4h		
4i		
4m		
4n		

4o

4s

Fig. 15. HOMO and LUMO of **4b**,**h**,**i**,**m**-**o**,**s**, calculated at CAM-B3LYP/aug-cc-pVTZ/IEF-PCM(UFF) level of theory (isovalue 0.02).

The electron distribution pattern is quite different in the case of compound **4s**. Electron density in the HOMO of triazole **4s** is mostly localized on the highly electron rich piperazinopyrimidine group at the C(5) position of the heterocycle. However, the LUMO is primarily localized on the central heterocyclic nucleus, the CN-group and the aromatic substituents, and there is little electronic density present on the piperazine group. Therefore, an intramolecular charge transfer process could be expected during an electron transition from the HOMO to the LUMO, resulting in fluorescence quenching. The theoretical predictions provide a robust interpretation of the experimental findings of the adsorption and emission maxima and are consistent with the trends in the experimentally determined quantum yields and emission shifts.

Quantitative evaluation of the charge distribution upon absorption and emission in triazoles **4** was determined by calculating the Mulliken's charges of the main moieties (triazole ring, aryl, R^1 and amino group) for molecules **4b**, **4h**, **4i**, **4j**, **4m**, **4n** and **4s** (Supporting Information, Table S3).

Charge distribution data for the triazole fragments for compounds **4b**, **4h**, **4i**, **4m**, **4n**, **4o** and **4s** provided an additional evidence for differences in their conjugation in the Frank-Condon state (S_{1v}) on one side and in the ground (S_0) or relaxed excited states (S_{1r}) on the other side. Substituents on the triazole ring and the aromatic cycle have a remarkable influence on the charge delocalization because their variation changes the spectral characteristics significantly. The most remarkable result is the large

33

increase in the sum of Mulliken's charges on the amino group at the C(5) atom of the triazole ring, especially for compounds **4h** and **4o**. Shifting of the pair of electrons on the amine nitrogen atom toward the triazole ring and subsequent increasing of the C-N bond order causes the C(5) atom to develop significant positive charge.

6. Conclusions

We have successfully designed and synthesized a series of small-molecule blue-light fluorophores based on the 2-aryl-5-amino-1,2,3-triazole scaffold. All investigated compounds showed strong absorption in UV, and the majority showed significant Stokes shifts upon emission. It is noteworthy that 2-aryltriazoles containing methoxy groups at the *N*(2) position of the triazole ring are the brightest fluorophores investigated, regardless of solvent. All of the triazoles exhibit solvent effects, and their emission increases dramatically in polar protic solvents such as ethanol. Many of these new 1,2,3-triazole derivatives had better fluorescence efficiency and larger Stokes shifts than those reported in the literature, making them attractive as potential fluorophores for technical and biological applications. Moreover, their structure can be easily modified to tune the maximum emission wavelength and quantum yield within the blue region to meet the application requirements.

These results suggest that the readily available 2-aryl-1,2,3-triazole chromophores could prove useful in electronic devices and as fluorescent probes. Finally, the biological stability of the triazole skeleton, the facile synthetic strategy, the economic competitiveness and the tuneable photophysical properties make 2-aryl-1,2,3-triazoles promising fluorophores for bioimaging and fluorescent labelling of biomolecules and cells.

Supplementary Data

Supplementary Data related to this article can be found at http://

References

[1]   Valeur B, Berberan-Santos MN. Molecular Fluorescence. 2nd ed. Weinhheim, Germany: Wiley-VCH Verlag & Co.; 2013.

[2]   Lakowicz JR. Principles of Fluorescence Spectroscopy. 3d ed. Maryland: Springer; 2006.

[3]   Ma N, Wang Y, Zhao BX, Ye WC, Jiang S. The application of click chemistry in the synthesis of agents with anticancer activity. Drug Des Devel Ther 2015;9:1585-99.

[4]   de Carvalho da Silva F, do Carmo Cardoso MF, Ferreira PG, Ferreira VF. Biological properties of 1*H*- and 2*H*-1,2,3-Triazoles. Top Heterocycl Chem 2015;40:117-166.

[5]   Ghosh D, Rhodes S, Hawkins K, Winder D, Atkinson A, Ming W, Padgett C, Orvis J, Aiken K., Landge S. A simple and effective 1,2,3-triazole based "turn-on" fluorescence sensor for the detection of anion. New J Chem 2015;39:295-303.

[6]   Schulze B, Schubert US. Beyond click chemistry – supramolecular interactions of 1,2,3-triazoles. Chem Soc Rev 2014;43: 2522-71.

[7]   Watkinson M. Click Triazoles as Chemosensors. Top Heterocycl Chem 2012;28:109-38.

[8]   Zheng T, Rouhanifard SH, Jalloh AS, Wu P. Click Triazoles for Bioconjugation. Top Heterocycl Chem 2012;28:163-184.

[9]   Sokolova NV, Nenajdenko VG. Recent advances in the Cu(I)-catalyzed azide–alkyne cycloaddition: focus on functionally substituted azides and alkynes. RSC Adv 2013:16212-16242.

[10] Belskaya N, Subbotina J, Lesogorova S. Synthesis of 2*H*-1,2,3-Triazoles. Top Heterocycl Chem 2015;40:51-116.

[11] Singh H, Sidhu J, Khurana JM. Synthesis and photophysical properties of novel chloroquinoline based chalcone derivates containing 1,2,3-triazole moiety. J Luminescence 2015;158:340-350.

[12] Katan C, Savel P, Wong BM, Roisnel T, Dorcet V, Jean-Luc Fillaut JL, Jacquemin D. Absorption and fluorescence signatures of 1,2,3-triazole based regioisomers: challenging compounds for TD-DFT. Phys Chem Chem Phys 2014;16:9064-73.

[13] Singh H, Sindhu J, Khurana JM, Sharma C, Aneja KR. Ultrasound promoted one pot synthesis of novel fluorescent triazolyl spirocyclic oxindoles using DBU based task specific ionic liquids and their antimicrobial activity. Eur J Med Chem 2014;77:145-54.

[14] Singh H, Sindhu J, Khurana JM. Determination of dipole moment, solvatochromic studies andapplication as turn off fluorescence chemosensor of new 3-(4-(dimethylamino)phenyl)-1-(5-methyl-1-(naphthalen-1-yl)-1*H*-1,2,3-triazol-4-yl)prop-2-en-1-one. Sensors and Actuators B 2014;192:536–542.

[15] Zhang Y, Ye X, Petersen JL, Li M, Shi X. Synthesis and characterization of Bis-N-2-Aryl Triazole as a fluorophore. J Org Chem 2015;80:3664-9.

[16] Padalkar VS, Lanke SK, Chemate SB, Sekar N. N-2-Aryl-1,2,3-Triazoles: A Novel Class of Blue Emitting Fluorophores-Synthesis, Photophysical Properties Study and DFT Computations. J Fluoresc 2015;25:985-96.

[17] Yan W, Wang Q, Lin Q, Li M, Petersen JL, Shi X. N-2-Aryl-1,2,3-triazoles: A Novel Class of UV/Blue-Light-Emitting Fluorophores with Tunable Optical Properties. Chem Eur J 2011;17:5011-18.

[18] Liu Y, Yan W, Chen Y, Petersen JL, Shi X. Efficient Synthesis of N-2-Aryl-1,2,3-Triazole Fluorophores via Post-Triazole Arylation. Org Lett 2008;105389-92.

[19] Gavlik KD, Sukhorukova ES, Lesogorova SG, Subbotina JO, Slepukhin PA, Benassi E. Synthesis of 2-Aryl-1,2,3-triazoles by Oxidative Cyclization of 2-(Arylazo)ethene-1,1-diamines: New One-pot Approach. Eur J Org Chem 2016; 2700-10.

[20] Bel'skaya NP, Demina MA, Sapognikova SG, Fan ZJ, Zhan HK, Dehaen W, Bakulev VA. Arkivoc 2008;*xvi*:9-21.

[21] Melhuish WH. Quantum efficiencies of fluorescence of organic substances: effect of solvent and concentration of the fluorescent solute. J Phys Chem 1961;65:229-35.

[22] Dolomanov OV, Bourhis LJ, Gildea RJ, Howard JAK, Puschmann H. OLEX2: a complete structure solution, refinement and analysis program. J Appl Cryst 2009;42:339-341.

[23] SHELXS, Sheldrick GM. Acta Cryst 2008;A64:112-122.

[24] SHELXL, Sheldrick GM. Acta Cryst 2008;A64:112-122.

[25] Becke AD. Density-functional thermochemistry. III. The role of exact exchange. J Chem Phys 1993;98:5648–5652.

[26] Zhao Y, Truhlar DG. The M06 suite of density functionals for main group thermochemistry, thermochemical kinetics, noncovalent interactions, excited states, and transition elements: two new functionals and systematic testing of four M06-class functionals and 12 other functionals.Theor Chem Acc 2008;120:215-241.

[27] Yanai T, Tew D, Handy N. A new hybrid exchange–correlation functional using the Coulomb-attenuating method (CAM-B3LYP). Chem Phys Lett 2004;393:51-57.

[28] Chai J–D, Head–Gordon MJ. Systematic optimization of long-range corrected hybrid density functionals. Chem Phys 2008;128:084106-1 – 084106-15.

[29] Dunning Jr. TH. Gaussian basis sets for use in correlated molecular calculations. I. The atoms boron through neon and hydrogen. J Chem Phys 1989;90:1007-1023.

[30] Kendall RA, Dunning Jr. TH, Harrison RJJ. Electron Affinities of the First-Row Atoms Revisited. Systematic Basis Sets and Wave Functions. Chem Phys 1992;96:6796-6806.

[31] Woon DE, Dunning Jr. TH. Gaussian Basis Sets for Use in Correlated Molecular Calculations. III. The second row atoms, Al-Ar. J Chem Phys 1993;8:1358-1371.

[32] Peterson KA, Woon DE, Dunning Jr. TH. Benchmark calculations with correlated molecular wave functions. IV. The classical barrier height of the $H + H_2 \rightarrow H_2 + H$ reaction. J Chem Phys 1994;100:7410-7415.

[33] Wilson AK, van Mourik T, Dunning Jr. TH. Gaussian basis sets for use in correlated molecular calculations. VI. Sextuple zeta correlation consistent basis sets for boron through neon. J Mol Struct Theochem 1996;388:339-349.

[34] Tomasi J, Mennucci B, Cancès E. The IEF version of the PCM solvation method: an overview of a new method addressed to study molecular solutes at the QM ab initio level J Mol Struct: Theochem 1999;464:211-226.

[35] Rappé AK, Casewit CJ, Colwell KS, Goddard WA, Skiff WM. UFF, a full periodic table force field for molecular mechanics and molecular dynamics simulations. J Am Chem Soc 1992;114:10024-10035.

[36] Frisch MJ, Trucks GW, Schlegel HB, Scuseria GE, Robb MA, Cheeseman JR, Scalmani G, Barone V, Mennucci B, Petersson GA et al., GAUSSIAN09, Revision D.01, Gaussian, Inc., Wallingford CT, 2009.

[37] Lide DR. CRC handbook of chemistry and physics, 96th Edition, Tailor & Francis, 2009 Bonds lengths in crystalline Organic compounds. 9-1-9-16.

- One-pot synthesis of a series of new 2-aryl-5-amino-1,2,3-triazole derivatives;

- Experimental and computational approaches to optical properties correlate well;

- High photoluminescence quantum yield (99.6%) was achieved;

- Fluorescent properties can be tuned varying the substituents in 1,2,3-triazoles.